Bifurcation analysis in 1D diffusive neural fields models with transmission delays

Riccardo Bellingacci
4282493
Utrecht University
February 5, 2017

Research project done in partial fulfillment of the requirements for the degree of Master of Mathematical Science at Utrecht University.

Supervisors: Stephan van Gils
Yuri A. Kuznetsov
Paul. A. Zegeling

Acknowledgements

This research project marks the end of my university studies and the beginning of a new life segment, thus I would like to thank: Stephan van Gils for his constant support and availability; I always left his office with a positive feeling; Yuri A. Kuznetsov for not only being my Tutor during the whole master but also for having me introduced to Stephan and co-supervised the thesis; Paul Zegeling for having agreed on being my third supervisor. Further I would like to thank Koen Dijkstra for having had the patience of helping me out on issues even though he was in the final months of his PhD. thesis; I wish you all the best.

My whole Utrecht experience has been strongly shaped by my flat mates Lina and Emanuele; words cannot describe how much energy you gave me during this quest. On days where nothing seemed to work, coming home to you was always a comfort and a reason to smile.
Nobody was as interested in the thesis as Felix. His constant support and curiosity in a subject which is not his own gave me always extra motivation and only few days passed without me meeting him. I would also like to thank Moritz; I could feel his positive energy from Munich to here; he was always very near even being physically very far.

Last but not least I would like to thank my parents. Any comment here would be an understatement to the fundamental role you always played in my life. This thesis is for you.

Contents

1 Introduction

Due to the massive amounts of neurons present in human brains (10^{11}), many difficulties arise when trying to model single neurons in a network of spiking neurons. It became hence a popular approach to consider a continuous space and spiking rates of neurons. This approach was largely introduced in the 1970s by the works of Wilson and Cowan [11],[12], Nunez [13] and Amari [14]; the models were called neural fields equations.

Amari focussed especially on mixed population models in interacting excitatory and inhibitory neurons, with a Mexican hat connectivity function; furthermore he formulated a voltage based model for activity with a sigmoidal firing rate function. These models where formulated as integro-differential equations and studied intensively in the succeeding years. For example, taking into consideration the natural delays that arise in the brain, due to the finite velocity of the impulses, the neural fields equations where modified into delay differential equations. Gils et al. [1] recently developed a local bifurcation theory for a class of abstract delay differential equations that cover neural field equations. Dijkstra et al. [2], later, showed how the computation done by Gils could be simplified if an odd sigmoidal firing rate function would be considered and symmetry arguments applied. In this paper spatial diffusion has been further added to the neural fields equations. Using the symmetries arguments presented in [2], local bifurcation theory with examples taken from both [1] and [2] will be analysed and the influence of diffusion on the solutions studied.

2 General Model

We will study the evolution of the synaptic current of a single population of neurons affected by spatial diffusion in a bounded open domain $\Omega \subset \mathbb{R}$, described by the system

$$\begin{aligned} \frac{\partial V}{\partial t}(t,x) &= D\frac{\partial^2 V}{\partial x^2}(t,x) - \alpha V(t,x) + \int_\Omega J(x,y)S(V(t-\tau(x,y),y))dy, \\ D\frac{\partial V}{\partial x}(t,x) &= 0, \qquad \text{for } t>0, \text{ on } x \in \partial\Omega. \end{aligned} \tag{NFE}$$

For neurons positioned at a point $x \in \overline{\Omega}$, let $V(t,x)$ be their averaged pre-synaptic membrane potential at time $t > 0$. The synaptic decay rate is given by $\alpha > 0$ and D is the diffusion coefficient. The spatial diffusion acts on the synaptic currents, hence we can consider it as an electrical current diffusion on the interval $(-1,1)$. The time it takes for a signal to travel from a neuron at location $y \in \Omega$ to a neuron at location

$x \in \Omega$ is described by the propagation delay $\tau(x, y)$, with $\tau \in C(\overline{\Omega} \times \overline{\Omega})$. Obviously, being a time measure, $\tau > 0$, holds, furthermore we define $h := \sup_{(x,y)\in\Omega} \tau(x, y)$ as the maximal delay and assume that this is a finite number. The strength of the neural signal is given by $J \in C(\overline{\Omega} \times \overline{\Omega})$. The firing rate of the neurons is given by the function $S \in C^\infty(\mathbb{R})$ and, by assumption, its k-th derivative is bounded. It follows that $S(V(t, x))$ describes the averaged firing rate of neurons at position $x \in \Omega$ and time t, given its pre-synaptic membrane potential $V(t, x)$. Furthermore, by setting $S(0) = 0$, $V(t, x)$ represents the deviation from the background state potential.

We use Neumann boundary condition because there is no flux at the boundary. Furthermore it is necessary to multiply the Neumann condition times D, such that for $D = 0$, the system (NFE) corresponds to system (NFE,[2]).

Now let $Y := \{y \in C^2(\overline{\Omega}) \,|\, y'(\partial\Omega) = 0\}$ and $X := C([-h, 0]; Y)$. For notational simplicity, define the non-linear operator $G : X \to Y$ as

$$G(\phi)(x) := \int_{\Omega} J(x, y)S(\phi(t - \tau(x, y), y))dy \qquad \forall \phi \in X, \, \forall x, y \in \overline{\Omega}. \tag{1}$$

From ([1], Proposition 11) it follows that G is well defined by (1) and that $G \in C^\infty(X, Y)$. Of course G depends on S and for $S = 0$ it follows that $G(0)$. We will analyse with greater care the function S later in this section. For $k \in \mathbb{N}$, the operator G is $k-$times Frechet differentiable with its derivative at a point $\phi \in X$ given by

$$(D^k G(\phi)(\varphi_1, \ldots, \varphi_k))(x) = \int_{\Omega} J(x, y)S^{(k)}(\phi(-\tau(x, y), y)) \prod_{i=1}^{k} \varphi_i(-\tau(x, y), y)dy \tag{2}$$

with $(\varphi_1, \ldots, \varphi_k) \in X$ and $x \in \overline{\Omega}$.

Hence we will work with following system

$$\begin{cases} \dot{V}(t) = D\frac{d^2}{dx^2}V_t(0) - \alpha V_t(0) + G(V_t) & \text{for } t \geq 0, x \in \overline{\Omega} \\ D\frac{\partial V}{\partial x}(t, x) = 0 \quad \text{for } t \geq 0 \text{ on } \partial\Omega, \\ V(t) = \phi(t) \quad \text{for } t \in [-h, 0] \end{cases} \tag{3}$$

with $\phi(t)$ being the initial condition of the problem and

$$V_t(\theta) := V(t + \theta) \qquad \forall t \geq 0, \text{ and } \theta \in [-h, 0].$$

The aim of this thesis is to deliver an explicit characterization of the normal forms occurring at bifurcation points. The first step will therefore be to deliver a detailed spectral analysis of the problem. For this, the system (NFE) needs to be linearised around its trivial equilibrium which yields the characteristic equation and polynomial. The roots of the characteristic polynomial are the eigenvalues of the problem; various symmetry arguments will facilitate the computation of the eigenvalues.

2.1 $\mathbb{Z}_2$ symmetries

For the non-diffusive problem, [2] has shown the presence of symmetries. More precisely due to the choice of an odd firing rate $\mathbb{Z}_2$-symmetries are generated by involutions $\kappa_{1,2} \in \mathcal{L}(Y)$ defined by

$$(\kappa_1 f)(x) := f(-x), \qquad (\kappa_2 f)(x) := -f(-x). \tag{4}$$

The fixed subspaces of the involutions κ_1 and κ_2 are composed of even and odd functions respectively. Now, if $\tilde{\kappa}_{1,2} \in \mathcal{L}(Y)$ are involutions defined by

$$(\tilde{\kappa}_1 \phi)(\theta, x) := \phi(\theta)(-x), \qquad (\tilde{\kappa}_2 \phi)(\theta, x) := -\phi(\theta)(-x), \tag{5}$$

then the (NFE) has the symmetries

$$\kappa_i F(\phi) = F(\tilde{\kappa}_i \phi). \tag{6}$$

The addition of diffusion does not change the above mentioned symmetry arguments and hence we can use the same methods used in [2].

3 Characteristic Equation

Let A be the infinitesimal generator of the solution semi-group, the standard notation will be used when discussing spectral theory, where $\rho(A) \subset \mathbb{C}$, $\sigma(A)$ and $\sigma_p(A)$ are the resolvent set, the spectrum and the point spectrum of A, respectively. As usual for $z \in \rho(A)$, $R(z, A) = (z - A)^{-1}$ denotes the resolvent of A at z.
In this thesis only one dimensional problems will be considered. The delay is composed by two parts: the conductance delay caused by the finite propagation speed of the action potentials and an "intrinsic" delay τ_0 caused by synaptic processes and dendritic integration. Space and time is rescaled such that $\overline{\Omega} = [-1, 1]$. All together we get

$$\frac{\partial V}{\partial t}(t, x) = D\frac{\partial^2 V}{\partial x^2}(t, x) - \alpha V(t, x) + \int_{-1}^{1} J(x, y)S(V(t - \tau(x, y), y))dy, \tag{7}$$

with

$$\tau(x, y) = \tau_0 + |x - y|, \quad \forall x, y \in \overline{\Omega}\,. \tag{8}$$

The function $S : \mathbb{R} \to (0, 1)$ is defined in [8] as an odd function

$$S(z) = \frac{1}{1 + e^{-rz}} - \frac{1}{2}, \tag{9}$$

with $r > 0$ being the steepness of the firing rate function. Furthermore, we chose J to be homogeneous, isotropic and given by a linear combination of $N \in \mathbb{N}$ exponentials [1]:

$$J(x, y) = \hat{J}(x - y) = \sum_{j=1}^{N} c_j e^{-\mu_j |x-y|}, \qquad \forall x, y \in (-1, 1), \tag{10}$$

where $c_j, \mu_j \in \mathbb{C}$ are chosen such that J is real. Further define following set:

$$\varsigma := \left\{ z \in \mathbb{C} : \exists l, j \in \{1, \dots, N\},\, l \neq j \text{ such that } k_l^2 = k_j^2 \right\}. \tag{11}$$

Here $k_i := z + \mu_i$ and $c_j := \hat{c}_j \cdot S'(0) = \hat{c}_j \cdot \frac{r}{4}$. Linearising (7) around the trivial equilibrium yields the characteristic equation

$$\Delta(z) q = 0, \tag{12}$$

where $\Delta(z) : Y \to Y$ is defined as follows

$$(\Delta(z)q)(x) = (z + \alpha) q(x) - D \frac{d^2}{dx^2} q(x) - \int_{-1}^{1} \hat{J}(x - y) e^{-z\tau_0} e^{-z|x-y|} q(y) dy. \tag{13}$$

Before further computations two known propositions taken from [1] but also valid for the diffusive case will be stated.

Proposition 1. *([[1], Proposition 21]). All solutions $q \in Y$ of the equation $(\Delta(z)q)(x) = 0$ are in fact in $C^\infty(\overline{\Omega})$.* □

Proposition 2. *([[4], Proposition VI.6.7]). The complex number $z \in \sigma(A)$ if and only if $0 \in \sigma(\Delta(z))$ and $\psi \in D(A)$ is an eigenfunction corresponding to z if and only if $\psi = \{\theta \mapsto e^{\theta z} q_z\}$ where the non-trivial $q_z \in Y$ satisfies $\Delta(z) q_z = 0$.* □

Theorem 3. *([[1], Proposition 25]). Whenever $z \notin \varsigma$, $(\Delta(z)q(x)) = 0$ implies*

$$\beta_{N+1} q_z^{(2N+2)} + \beta_N q_z^{(2N)} + \cdots + \beta_1 q_z^{(2)} + \beta_0 q_z = 0, \tag{14}$$

for some unique vector $\beta \in \mathbb{C}^{N+1}$ depending on z and $q_z^{(k)}$ denoting the k-th derivative of q_z with respect to the spatial variable. □

Eigenvalues of the linear ODE (14) are roots of the characteristic polynomial $\mathcal{P}_z$ given by the following proposition:

Proposition 4. *For $z \notin \varsigma$ the characteristic polynomial $\mathcal{P}_z$ of (14) is given by*

$$\mathcal{P}_z(\rho) = (z+\alpha)e^{z\tau_0}\prod_{i=1}^{N}\left(\rho^2 - k_i^2\right) - De^{z\tau_0}\rho^2\prod_{i=1}^{N}\left(\rho^2 - k_i^2\right) - 2\sum_{i=1}^{N}c_i k_i \prod_{\substack{j=1\\ j\neq i}}^{N}\left(\rho^2 - k_i^2(z)\right). \tag{15}$$

Proof. First define

$$\mathcal{L}_i := \left(\partial_x^2 - k_i^2(z)\right), \tag{16}$$

and

$$K := \sum_{i=1}^{N} K_i, \quad \text{with} \quad K_i(q)(z) := \int_\Omega c_i e^{-(\mu_i+z)|x-y|}e^{-z\tau_0}q(y)dy, \tag{17}$$

for all $i = 1, \dots, N$.
Notice now that

$$\partial_x^2 e^{-(\mu_i+z)|x-y|} = \partial_x^2 e^{-k_i|x-y|} = [k_i^2 - 2k_i\delta(x-y)]e^{\partial_x^2 e^{-k_i|x-y|}}, \tag{18}$$

and hence

$$\begin{aligned} \mathcal{L}_j(K_j(q)(z)) &= -k_j^2\int_\Omega c_j e^{-k_j|x-y|}e^{-z\tau_0}q(y) + c_j[k_j^2 - 2k_j\delta(x-y)]e^{-k_j|x-y|}e^{-z\tau_0}q(y)dy \\ &= -2c_j k_j \int_\Omega e^{-k_j|x-y|}e^{-z\tau_0}q(y). \end{aligned} \tag{19}$$

so applying all different $\mathcal{L}_\rangle$ to (13) yields the following ODE

$$\left[(z+\alpha)e^{z\tau_0}\prod_{i=1}^{N}\mathcal{L}_i - De^{z\tau_0}\,\partial_x^2\prod_{i=1}^{N}\mathcal{L}_i - 2\sum_{i=1}^{N}c_i k_i\prod_{\substack{j=1\\ j\neq i}}^{N}\mathcal{L}_i\right]q. \tag{20}$$

Hence the characteristic polynomial is

$$\mathcal{P}_z(\rho) = (z+\alpha)e^{z\tau_0}\prod_{i=1}^{N}\left(\rho^2 - k_i^2\right) - De^{z\tau_0}\rho^2\prod_{i=1}^{N}\left(\rho^2 - k_i^2\right) - 2\sum_{i=1}^{N}c_i k_i \prod_{\substack{j=1\\ j\neq i}}^{N}\left(\rho^2 - k_i^2(z)\right). \tag{21}$$

□

By adding diffusivity, the characteristic polynomial increases of two orders with respect to the non-diffusive case, thus there will be a pair of roots, hence a pair of eigenvalues, more than in [2].

Proposition 5. *If the characteristic polynomial $\mathcal{P}_z(\rho)$ has $2N+2$ distinct roots for some $z \in \mathbb{C}$, then $k_l(z) \neq 0$ for all $l = 1, \dots, N$.*

Proof. Assume that $k_l(z) = 0$ for some $l = 1, \dots, N$, then without loss of generality set $l = N$, then the characteristic polynomial becomes

$$\begin{aligned}\mathcal{P}_z(\rho) = (z+\alpha)e^{z\tau_0}\rho^2 \prod_{i=1}^{N-1}\left(\rho^2 - k_i^2\right) - De^{z\tau_0}\rho^4 \prod_{i=1}^{N-1}\left(\rho^2 - k_i^2\right) \\ - 2\sum_{i=1}^{N-1} c_i k_i \prod_{\substack{j=1\\ j\neq i}}^{N-1}\left(\rho^2 - k_j^2(z)\right)\rho^2.\end{aligned} \tag{22}$$

Clearly ρ^2 is a common factor of the characteristic polynomial, hence a double root at $\rho = 0$ must exist. However the order of the polynomial is $2N+2$, meaning that it should have $2N$ roots away from 0; hence $k_i(z) \neq 0$ for all $i = 1, \dots, N$. □

Proposition 6. *Let $z \notin \varsigma$ and if the characteristic polynomial has $2N+2$ distinct roots $\pm\rho_1, \dots, \pm\rho_{N+1}$, then $k_j(z) \neq \pm\rho_m$, for all $m = 1, \dots, N+1$ and $j = 1, \dots, N$.*

Proof. Clearly if $\mathcal{P}_z(k_l) \neq 0$ for all $l = 1, \dots, N$, then k_l is not a root and hence $k_j(z) \neq \pm\rho_m$. We must hence show $\mathcal{P}_z(k_l) \neq 0$. Without loss of generality let $l = N$, then the characteristic polynomial takes following form

$$\begin{aligned}\mathcal{P}_z(k_N) &= (z+\alpha)e^{z\tau_0} \prod_{i=1}^{N}\left(k_N^2 - k_i^2\right) - De^{z\tau_0}k_N^2 \prod_{i=1}^{N}\left(k_N^2 - k_i^2\right) \\ &\quad - 2\sum_{i=1}^{N} c_i k_i \prod_{\substack{j=1\\ j\neq i}}^{N}\left(k_N^2 - k_j^2(z)\right) \\ &= -2c_N \cdot k_N \prod_{j=1}^{N-1}(k_N^2 - k_j^2).\end{aligned} \tag{23}$$

By definition $c_N \neq 0$ and from the previous proposition we know that $k_N \neq 0$ and hence $\mathcal{P}_z(k_l) \neq 0$. □

Lemma 7. *If $z \notin \varsigma$ and the characteristic polynomial $\mathcal{P}_z$ has $2N+2$ distinct roots $\pm\rho_1(z), \dots, \pm\rho_{N+1}(z)$, then the general solution to (13) is of the form*

$$q_z(x) = \sum_{i=1}^{N+1}\left[a_i \cosh(\rho_i(z)x) + b_i \sinh(\rho_i(z)x)\right], \tag{24}$$

where the coefficients a_i, $b_i \in \mathbb{C}$ are arbitrary. □

Theorem 8. *Suppose that $z \notin \varsigma$ and the characteristic polynomial $\mathcal{P}_z$ has $2N+2$ distinct roots denoted by $\pm\rho_i(z)$ for $i = 1, \ldots, N+1$, then z is an eigenvalue of A if and only if*

$$\det \begin{bmatrix} \hat{S}_z^e \\ [\rho_i \sinh(\rho_i)]_i \end{bmatrix} \det \begin{bmatrix} \hat{S}_z^o \\ [\rho_i \cosh(\rho_i)]_i \end{bmatrix} = 0. \tag{25}$$

Furthermore, $\{\theta \mapsto e^{\theta z} q_z\} \in X$ is a corresponding eigenfunction with $q_z \in Y$ as in (24). If (25) holds then the coefficients $a = [a_1, a_2, \ldots, a_{N+1}]$ and $b = [b_1, b_2, \ldots b_{N+1}]$ are a non-trivial solution of the system of equations

$$\begin{bmatrix} \hat{S}_z^e & 0 \\ [\rho_i \sinh(\rho_i)]_i & 0 \\ 0 & [\rho_i \cosh(\rho_i)]_i \\ 0 & \hat{S}_z^o \end{bmatrix} \begin{bmatrix} a \\ b \end{bmatrix} = 0, \tag{26}$$

Remarks

- $\hat{S}_z^e$ and $\hat{S}_z^o$ will be defined more precisely later on, in the proof.
- $[\rho_i \sinh(\rho_i)]_i$ and $[\rho_i \cosh(\rho_i)]_i$ are vectors of length $N+1$ and are both derived from the Neumann boundary condition, as it will be shown later in the proof.
- To determine the exact solution it is necessary to compute the coefficients $a := [a_1, \ldots, a_{N+1}]$ and $b := [b_1, \ldots, b_{N+1}]$. Proposition 2 gives a necessary condition these coefficients need to full-fill

Proof.
Inserting q_z into (13) and using (10), gives

$$\begin{aligned} 0 = &(z+\alpha)e^{z\tau_0} \sum_{i=1}^{N+1} [a_i \cosh(\rho_i(z)x) + b_i \sinh(\rho_i(z)x)] \\ &- De^{z\tau_0} \frac{d^2}{dx^2} (\sum_{i=1}^{N+1} [a_i \cosh(\rho_i(z)x) + b_i \sinh(\rho_i(z)x)]) \\ &+ \sum_{j=1}^{N} c_j \int_{-1}^{1} e^{-k_j(z)|x-y|} \sum_{i=1}^{N+1} [a_i \cosh(\rho_i(z)y) + b_i \sinh(\rho_i(z)y)] \, dy. \end{aligned} \tag{27}$$

The second derivative can be easily calculated as follows

$$\frac{d^2}{dx^2} (\sum_{i=1}^{N+1} [a_i \cosh(\rho_i x) + b_i \sinh(\rho_i x)]) = (\sum_{i=1}^{N+1} \left[a_i \rho_i^2 \cosh(\rho_i x) + b_i \rho_i^2 \sinh(\rho_i x)\right]). \tag{28}$$

Integrating by parts and splitting (27) gives

$$
\begin{aligned}
0 = \sum_{i=1}^{N+1} \Bigg\{ & a_i \cosh(\rho_i x) \left[e^{z\tau_0}(z+\alpha) - \sum_{j=1}^{N} \frac{2c_j k_j}{k_j^2 - \rho_i^2} \right] \\
& + b_i \sinh(\rho_i x) \left[e^{z\tau_0}(z+\alpha) - \sum_{j=1}^{N} \frac{2c_j k_j}{k_j^2 - \rho_i^2} \right] \Bigg\} \\
& - De^{z\tau_0} \Big(\sum_{i=1}^{N+1} \left[a_i \rho_i^2 \cosh(\rho_i x) + b_i \rho_i^2 \sinh(\rho_i x) \right] \Big) \\
& + \sum_{j=1}^{N} c_j e^{-k_j} \Bigg\{ e^{k_j x} \left[\sum_{i=1}^{N+1} a_i \left[S_z^e \right]_{j,i} + \sum_{i=1}^{N+1} b_i \left[S_z^o \right]_{j,i} \right] \\
& + e^{-k_j x} \left[\sum_{i=1}^{N+1} a_i \left[S_z^e \right]_{j,i} + \sum_{i=1}^{N+1} b_i \left[S_z^o \right]_{j,i} \right] \Bigg\},
\end{aligned}
\tag{29}
$$

where the dependency on z has been omitted when obvious, and

$$
\begin{aligned}
\left[\hat{S}_z^e \right]_{j,i} &:= \frac{k_j(z) \cosh(\rho_i(z)) + \rho_i(z) \sinh(\rho_i(z))}{k_j(z)^2 - \rho_i(z)^2}, \\
\left[\hat{S}_z^o \right]_{j,i} &:= \frac{k_j(z) \sinh(\rho_i(z)) + \rho_i(z) \cosh(\rho_i(z))}{k_j(z)^2 - \rho_i(z)^2},
\end{aligned}
\tag{30}
$$

with $i = 1, \ldots, N+1$ and $j = 1, \ldots, N$.
The expression (29) can be rewritten as

$$
\begin{aligned}
0 = \sum_{i=1}^{N+1} \Bigg\{ & a_i \cosh(\rho_i x) \left[e^{z\tau_0}(z+\alpha) - \sum_{j=1}^{N} \frac{2c_j k_j}{k_j^2 - \rho_i^2} - De^{z\tau_0} \rho_i^2 \right] \\
& + b_i \sinh(\rho_i x) \left[e^{z\tau_0}(z+\alpha) - \sum_{j=1}^{N} \frac{2c_j k_j}{k_j^2 - \rho_i^2} - De^{z\tau_0} \rho_i^2 \right] \Bigg\} \\
& + \sum_{j=1}^{N} c_j e^{-k_j} \Bigg\{ e^{k_j x} \left[\sum_{i=1}^{N+1} a_i \left[\hat{S}_z^e \right]_{j,i} + \sum_{i=1}^{N+1} b_i \left[\hat{S}_z^o \right]_{j,i} \right] \\
& \qquad + e^{-k_j x} \left[\sum_{i=1}^{N+1} a_i \left[\hat{S}_z^e \right]_{j,i} + \sum_{i=1}^{N+1} b_i \left[\hat{S}_z^o \right]_{j,i} \right] \Bigg\}.
\end{aligned}
\tag{31}
$$

The first part of (31) is equal to 0 iff

$$
\left[e^{z\tau_0}(z+\alpha) - \sum_{j=1}^{N} \frac{2c_j k_j}{k_j^2 - \rho_i^2} - De^{z\tau_0} \rho_i^2 \right] = 0. \tag{32}
$$

Now a quick computation shows

$$\begin{aligned}\sum_{j=1}^{N}\frac{2c_jk_j}{k_j^2-\rho_i^2}\prod_{j=1}^{N}\left[k_j^2-\rho_i^2\right] &= \frac{2c_1k_1}{k_1^2-\rho_i^2}\prod_{j=1}^{N}\left[k_j^2-\rho_i^2\right]+\frac{2c_2k_2}{k_2^2-\rho_i^2}\prod_{j=1}^{N}\left[k_j^2-\rho_i^2\right]+\dots\\ &= 2c_1k_1\prod_{j=2}^{N}\left[k_j^2-\rho_i^2\right]+2c_2k_2\prod_{\substack{j=1\\ j\neq 2}}^{N}\left[k_j^2-\rho_i^2\right]+\dots\\ &= \sum_{i=1}^{N}2c_ik_i\prod_{\substack{j=1\\ j\neq i}}^{N}\left[k_j^2-\rho_i^2\right],\end{aligned} \tag{33}$$

and hence multiplying (32) with $\prod_{j=1}^{N}\left[k_j^2-\rho_i^2\right]$ and using the above equation, gives

$$\begin{aligned}0 &= \prod_{j=1}^{N}\left[k_j^2-\rho_i^2\right]\left[e^{z\tau_0}(z+\alpha)-\sum_{j=1}^{N}\frac{2c_jk_j}{k_j^2-\rho_i^2}-De^{z\tau_0}\rho_i^2\right]\\ &= e^{z\tau_0}(z+\alpha)\prod_{j=1}^{N}\left[k_j^2-\rho_i^2\right]-\sum_{i=1}^{N}2c_ik_i\prod_{\substack{j=1\\ j\neq i}}^{N}\left[k_j^2-\rho_i^2\right]-De^{z\tau_0}\rho_i^2\prod_{j=1}^{N}\left[k_j^2-\rho_i^2\right],\end{aligned} \tag{34}$$

and then (32) holds because of Proposition 4. On the other hand considering $a := [a_1, a_2, \dots, a_{N+1}]$ and $b := [b_1, b_2, \dots, b_{N+1}]$, it is clear that the last line in (31) vanishes if and only if

$$\begin{bmatrix}\hat{S}_z^e & 0\\ 0 & \hat{S}_z^o\end{bmatrix}\begin{bmatrix}a\\ b\end{bmatrix}=0, \tag{35}$$

with $\hat{S} := \begin{bmatrix}\hat{S}_z^e & 0\\ 0 & \hat{S}_z^o\end{bmatrix}$, a $(2N)\times(2N+2)$ matrix and a, b as before.

The matrix $\tilde{S}$ is not quadratic. By taking into consideration the boundary condition the matrix can be made quadratic. From the Neumann boundary conditions it follows that

$$0 = D\frac{dV}{dx}\bigg|_{x=\pm1} = D\frac{d}{dx}e^{z\tau_0}q(x)\bigg|_{x=\pm1} = De^{z\tau_0}q'(x)\bigg|_{x=\pm1}, \tag{36}$$

hence

$$0 = De^{z\tau_0}\frac{d}{dx}q(x)\bigg|_{x=1} = De^{z\tau_0}\frac{d}{dx}\sum_{i=1}^{N+1}\left[a_i\cosh(\rho_i x) + b_i\sinh(\rho_i x)\right]$$
$$= De^{z\tau_0}\sum_{i=1}^{N+1}\left[a_i p_i\sinh(\rho_i) + b_i p_i\cosh(\rho_i)\right]. \tag{37}$$

Therefore in order for (37) to hold it follows that:

$$\begin{aligned}\left[\rho_i\sinh(\rho_i)\right]_i \cdot a = 0,\\ \left[\rho_i\cosh(\rho_i)\right]_i \cdot b = 0,\end{aligned} \tag{38}$$

with $\left[\rho_i\cosh(\rho_i)\right]_i$ and $\left[\rho_i\sinh(\rho_i)\right]_i$ $N+1$ vectors.
Plugging these two equations into (35) gives

$$\begin{bmatrix} \hat{S}_z^e & 0 \\ [\rho_i\sinh(\rho_i)]_i & 0 \\ 0 & [\rho_i\cosh(\rho_i)]_i \\ 0 & \hat{S}_z^o \end{bmatrix}\begin{bmatrix} a \\ b \end{bmatrix} = 0, \tag{39}$$

System (39), therefore, has a non trivial solution if and only if

$$\det\begin{bmatrix} \hat{S}_z^e \\ [\rho_i\sinh(\rho_i)]_i \end{bmatrix}\det\begin{bmatrix} \hat{S}_z^o \\ [\rho_i\cosh(\rho_i)]_i \end{bmatrix} = 0. \tag{40}$$

□

It is hence possible to determine the characteristic equation and to compute eigenvalues by solving (40). Depending whether

$$\det\begin{bmatrix} \hat{S}_z^e \\ [\rho_i\sinh(\rho_i)]_i \end{bmatrix} = 0, \tag{41}$$

or

$$\det\begin{bmatrix} \hat{S}_z^o \\ [\rho_i\cosh(\rho_i)]_i \end{bmatrix} = 0, \tag{42}$$

we say the eigenvalue is *even* or *odd*, respectively. The implementation will be carried forward using Matlab, later on.

4 Normal forms Coefficients

4.1 Andronov-Hopf Normal Forms

This part is entirely taken from [1] and only the results are repeated. In the case where $\sigma(A)$ contains only a simple pair of purely imaginary eigenvalues $\lambda_{1,2} = \pm i\omega_0$, with $\omega_0 > 0$ and no other eigenvalue on the imaginary axis, then the restriction of (NFE) on the critical centre manifold is smoothly equivalent to the *Poincarè Normal Form* given by

$$\dot{z} = i\omega_0 z + g_{21} z|z|^2 + \mathcal{O}(|z|^4). \tag{43}$$

Using the fact that S is an odd function one gets

$$g_{21} = \frac{1}{2}\langle \psi_1^{\odot}, C(\psi_1, \psi_1, \bar{\psi_1})\rangle = \frac{1}{2}\langle \psi_1^{\odot}, (y_{11}, 0)\rangle, \tag{44}$$

where

$$y_{11} := D^3G(0)(\psi_1, \psi_1, \bar{\psi_1}), \tag{45}$$

with $D^3G(0)$ described in (2) and ψ_1 being the eigenfunction normalized such that

$$< \psi_1^{\odot}, j\psi_1 >= 1. \tag{46}$$

4.2 Pitchfork-Hopf Normal Form

It has been shown in [2] that for a Pitchfork-Hopf bifurcation the restriction of (NFE) onto the critical centre manifold is equivalent to the symmetric normal form

$$\begin{cases} \dot{\omega} = g_{300}\omega^3 + g_{111}\omega|z|^2 + \mathfrak{O}(|\omega, z, \bar{z}|^5), \\ \dot{z} = i\omega z + g_{210} z w^2 + g_{021} z|z|^2 + \mathfrak{O}(|\omega, z, \bar{z}|^5), \end{cases} \tag{47}$$

where $\omega \in \mathbb{R}, z \in \mathbb{C}$ [9]. Using [[1], Lemma 33], [2] shows that

$$\begin{aligned} g_{300} &= \frac{1}{6}\langle \psi_1^{\odot}, C(\psi_1, \psi_1, \psi_1)\rangle = \frac{1}{6}\langle \psi_1^{\odot}, (y_{11}, 0)\rangle, \\ g_{111} &= \langle \psi_1^{\odot}, C(\psi_1, \psi_2, \bar{\psi_2})\rangle = \langle \psi_1^{\odot}, (y_{12}, 0)\rangle, \\ g_{210} &= \frac{1}{2}\langle \psi_2^{\odot}, C(\psi_2, \psi_1, \psi_1)\rangle = \frac{1}{2}\langle \psi_2^{\odot}, (y_{21}, 0)\rangle, \\ g_{021} &= \frac{1}{2}\langle \psi_2^{\odot}, C(\psi_2, \psi_2, \bar{\psi_2})\rangle = \frac{1}{2}\langle \psi_2^{\odot}, (y_{22}, 0)\rangle, \end{aligned} \tag{48}$$

where

$$\begin{aligned} y_{11} &:= D^3G(0)(\psi_1, \psi_1, \psi_1), \\ y_{12} &:= D^3G(0)(\psi_1, \psi_2, \bar{\psi_2}), \\ y_{21} &:= D^3G(0)(\psi_2, \psi_1, \psi_1), \\ y_{22} &:= D^3G(0)(\psi_2, \psi_2, \bar{\psi_2}), \end{aligned} \tag{49}$$

with $D^3G(0)$ described in (2).
It will be our aim to find the various values of the g's in (44) and (48) . The eigenfunction ψ_i for all $i = 1, 2$ is known and has been described in the section before; however it is not possible to calculate $\psi^{\odot}$ explicitly, where $\psi^{\odot}$ is one of the eigenfunctions . Nevertheless we know from [2] that for some $\nu \in \mathbb{C}$, following holds

$$\langle \psi^{\odot}, \phi^{\odot *} \rangle = \langle P^{\odot} \psi^{\odot}, \phi^{\odot *} \rangle \tag{50}$$

$$= \langle \psi^{\odot}, P^{\odot *} \phi^{\odot *} \rangle = \nu \langle \psi^{\odot}, j\psi \rangle = \nu, \tag{51}$$

and hence, taking g_{300} as an example, we get

$$g_{300} = \frac{1}{6} \langle \psi_1^{\odot}, (y_{11}, 0) \rangle = \frac{1}{6} \nu_{300}. \tag{52}$$

Clearly to calculate the normal forms coefficients we have to compute the specific ν. The following Lemma or a variant of it, is necessary when calculating ν. We are not sure how to define F and there are some functional analytical considerations to make, which will not be made here. A forthcoming paper in this topics is expected to be published soon.

Lemma 9. *Suppose that $z \in \rho(A)$. For each $y \in Y$ the function $\varphi = \{\theta \to e^{\theta z} \triangle(z)^{-1} y\}$ is the unique solution in $C^1([-h, 0]; Y)$ of the system*

$$\begin{cases} z\varphi(0) - DF(0)\varphi = y, \\ z\varphi - \varphi' = 0. \end{cases} \tag{53}$$

Moreover, $\varphi^{\odot *} = j\varphi$ is the unique solution in $D(A^{\odot *})$ of $(z - A^{\odot *})\varphi^{\odot *} = (y, 0)$, i.e $\varphi^{\odot *} = R(z, A^{\odot *})(y, 0)$. $\square$

Everything stated until now in this section, together with following equality

$$P^{\odot *} \phi^{\odot *} = \frac{1}{2\pi i} \oint_{\partial C_\lambda} R(z, A^{\odot *}) \phi^{\odot *} dz = \nu j \psi, \tag{54}$$

gives us following representation

$$\frac{1}{2\pi i} \oint_{\partial C_\lambda} \triangle(z)^{-1} y \, dz = \nu \psi(0), \tag{55}$$

with C_λ a sufficiently small open disk centred at λ.

5 Resolvent Equation

We notice that equation (55) describes a similar situation to the homogeneous case: it is necessary to solve an integral equation for $q_z := \triangle(z)^{-1}y \in Y$, which means solving the resolvent equation

$$(\Delta(z)q)(x) = (z+\alpha)q_z(x) - Dq_z''(x) - \int_{-1}^{1} \hat{J}_0(x-r)e^{-z\tau_0}e^{-z|x-r|}q_z(r)dr = y(x), \quad (56)$$

for all $x \in \bar{\Omega}$. Adjusting the previous ansatz to the inhomogeneous case, we take

$$q_z(x) = \frac{y(x)}{z+\alpha} + \sum_{i=1}^{N+1} \left[a_i(x)\cosh(\rho_i(z)x) + b_i(x)\sinh(\rho_i(z)x)\right], \quad (57)$$

as the general solution.
Note that both $a, b \in Y := \{y \in C^2(\overline{\Omega}) \,|\, y'(\partial\Omega) = 0\}$. They are not constants like in Lemma (7), but depend on x.

Inserting the solution (57) into the characteristic equation gives

$$
\begin{aligned}
0 = \sum_{i=1}^{N+1} \Bigg\{ & a_i(x)\cosh(\rho_i x) \left[e^{z\tau_0}(z+\alpha) - \sum_{j=1}^{N} \frac{2c_j k_j}{k_j^2-\rho_i^2} \right] \\
& + b_i(x)\sinh(\rho_i x) \left[e^{z\tau_0}(z+\alpha) - \sum_{j=1}^{N} \frac{2c_j k_j}{k_j^2-\rho_i^2} \right] \Bigg\} \\
& - D\cdot e^{z\tau_0} \cdot \Bigg(\frac{y''(x)}{z+\alpha} + \sum_{i=1}^{N+1} \left[a_i(x)\rho_i^2\cosh(\rho_i x) + b_i(x)\rho_i^2\sinh(\rho_i x) \right] \\
& + 2\rho_i \left[a_i'(x)\sinh(\rho_i x) + b_i'(x)\cosh(\rho_i x) \right] + \left[a_i''(x)\cosh(\rho_i x) + b_i''(x)\sinh(\rho_i x) \right] \Bigg) \\
& + \sum_{j=1}^{N} c_j e^{-k_j} \int_{-1}^{x} e^{k_j r} \left[\frac{-y(r)}{z+\alpha} + \sum_{i=1}^{N+1} \frac{a_i'(r)}{k_j^2-\rho_i^2} \times (k_j\cosh(\rho_i r) - \rho_i\sinh(\rho_i r)) \right. \\
& \left. + \sum_{i=1}^{N+1} \frac{b_i'(r)}{k_j^2-\rho_i^2} \times (k_j\sinh(\rho_i r) - \rho_i\cosh(\rho_i r)) \right] dr \\
& - \sum_{j=1}^{N} c_j e^{k_j} \int_{x}^{1} e^{-k_j r} \left[\frac{y(r)}{z+\alpha} + \sum_{i=1}^{N+1} \frac{a_i'(r)}{k_j^2-\rho_i^2} \times (k_j\cosh(\rho_i r) - \rho_i\sinh(\rho_i r)) \right. \\
& \left. + \sum_{i=1}^{N+1} \frac{b_i'(r)}{k_j^2-\rho_i^2} \times (k_j\sinh(\rho_i r) - \rho_i\cosh(\rho_i r)) \right] dr \\
& + \sum_{j=1}^{N} c_j e^{-k_j(1+x)} \left[\sum_{i=1}^{N+1} a_i(-1)\left[S_z^e\right]_{j,i} - \sum_{i=1}^{N+1} b_i(-1)\left[S_z^o\right]_{j,i} \right] \\
& + \sum_{j=1}^{N} c_j e^{-k_j(1-x)} \left[\sum_{i=1}^{N+1} a_i(1)\left[S_z^e\right]_{j,i} + \sum_{i=1}^{N+1} b_i(1)\left[S_z^o\right]_{j,i} \right],
\end{aligned}
\tag{58}
$$

where the dependence on z has been omitted when clear.
We have to find values of $a(x) := [a_1(x), \dots, a_{N+1}(x)]$ and $b(x) := [b_1(x), \dots, b_{N+1}(x)]$ such that the above equation is satisfied.

The first three lines in (58) can be rewritten in the form:

$$
\begin{aligned}
0 = \sum_{i=1}^{N+1} \Bigg\{ & a_i(x)\cosh(\rho_i x)\left[e^{z\tau_0}(z+\alpha) - \sum_{j=1}^{N} \frac{2c_j k_j}{k_j^2-\rho_i^2} - De^{z\tau_0}\rho_i^2\right] \\
& + b_i(x)\sinh(\rho_i x)\left[e^{z\tau_0}(z+\alpha) - \sum_{j=1}^{N} \frac{2c_j k_j}{k_j^2-\rho_i^2} - De^{z\tau_0}\rho_i^2\right]\Bigg\} \\
& - D\cdot e^{z\tau_0}\cdot\left(\frac{y''(x)}{z+\alpha} + \sum_{i=1}^{N+1} 2\rho_i\left[a_i'(x)\sinh(\rho_i x) + b_i'(x)\cosh(\rho_i x)\right]\right. \\
& \left. + \left[a_i''(x)\cosh(\rho_i x) + b_i''(x)\sinh(\rho_i x)\right]\right),
\end{aligned} \tag{59}
$$

and through Proposition 4 we know that the first part of (59) vanishes. The rest of (58) can be written as following system of equations:

$$
\begin{cases}
\hat{K}_z[A_z(x)a'(x) + B_z b'(x)] = 0, & \text{(60a)} \\
\hat{M}_z[B_z(x)a'(x) + A_z(x)b'(x)] = -\dfrac{y(x)}{z+\alpha}\mathbf{1}, & \text{(60b)} \\
\displaystyle\sum_{i=1}^{N+1} 2\rho_i\left[a_i'(x)\sinh(\rho_i x) + b_i'(x)\cosh(\rho_i x)\right] & \\
\qquad + \left[a_i''(x)\cosh(\rho_i x) + b_i''(x)\sinh(\rho_i x)\right] = -\dfrac{y''(x)}{z+\alpha}, & \text{(60c)}
\end{cases}
$$

with following boundary conditions derived from the last two lines of (58)

$$
\hat{S}_z^e a(1) + \hat{S}_z^o b(1) = 0, \tag{61}
$$

$$
\hat{S}_z^e a(-1) - \hat{S}_z^o b(-1) = 0. \tag{62}
$$

Here $\mathbf{1} \in \mathbb{R}^N$ is the vector with one at each entry, and for all $i = 1, \dots, N+1$ and $j = 1, \dots, N$

$$
[\hat{K}_z]_{j,i} := \frac{k_j(z)}{k_j(z)^2 - \rho_i(z)^2}, \qquad [\hat{M}_z]_{j,i} := \frac{\rho_i(z)}{k_j(z)^2 - \rho_i(z)^2}, \tag{63}
$$

and

$$
\begin{aligned}
A_z(x) &:= \begin{bmatrix} \cosh(\rho_1(z)x) & & 0 \\ & \ddots & \\ 0 & & \cosh(\rho_{N+1}(z)x) \end{bmatrix}, \\
B_z(x) &:= \begin{bmatrix} \sinh(\rho_1(z)x) & & 0 \\ & \ddots & \\ 0 & & \sinh(\rho_{N+1}(z)x) \end{bmatrix}.
\end{aligned} \tag{64}
$$

It is our aim now to find non trivial $a(x), b(x)$ that solve the above system. We first notice that both $\hat{K}$ and $\hat{M}$ are $N \times (N+1)$ matrices. For further computation it would be convenient to incorporate (60c) into $\hat{K}, \hat{M}$, making both matrices square; to do this we will reformulate equation (60c). Exploiting that for all $i = 1, \ldots, N+1$

$$a_i''(x)\cosh(\rho_i x) = (a_i'(x)\cosh(\rho_i x))' - \rho_i a_i' \sinh(\rho_i x),$$

and analogously

$$b_i''(x)\sinh(\rho_i x) = (b_i'(x)\sinh(\rho_i x))' - \rho_i b_i' \cosh(\rho_i x),$$

equation (60c) becomes

$$\sum_{i=1}^{N+1} \rho_i \left[a_i'(x)\sinh(\rho_i x) + b_i'(x)\cosh(\rho_i x)\right] \\ + \left[a_i'(x)\cosh(\rho_i x) + b_i'(x)\sinh(\rho_i x)\right]' = -\frac{y''(x)}{z+\alpha}. \tag{65}$$

At this stage we need the assumption that

$$\begin{cases} \sum_{i=1}^{N+1} \left[a_i'(x)\rho_i \sinh(\rho_i x) + b_i'(x)\rho_i \cosh(\rho_i x)\right] = 0, \\ \sum_{i=1}^{N+1} \left[a_i'(x)\cosh(\rho_i x) + b_i'(x)\sinh(\rho_i x)\right]' + \frac{y''(x)}{z+\alpha} = 0. \end{cases} \tag{66}$$

Rewriting the above system into matrix vector form gives

$$\begin{cases} \rho\big[A_z(x)b'(x) + B_z(x)a'(x)\big] = 0, \\ [\mathbf{1}^\top[A_z(x)a'(x) + B_z(x)b'(x)]]' + \frac{y''(x)}{z+\alpha} = 0, \end{cases} \tag{67}$$

where

$$\rho := [\rho_1, \ldots, \rho_{N+1}], \qquad \text{and} \qquad \mathbf{1}^\top := [1, \ldots, 1], \tag{68}$$

$(N+1)$ vectors. From the second equation of system (67) we derive

$$\mathbf{1}^\top[A_z(x)a'(x) + B_z(x)b'(x)] + \frac{y'(x)}{z+\alpha} = C, \tag{69}$$

for a $C \in \mathbb{R}$ and all $x \in \overline{\Omega}$. (69) holds for all $x \in \overline{\Omega}$, hence also for $x = 1$. Because $a, b, y \in Y$ we know that $a'(1) = b'(1) = y'(1) = 0$; it then follows that

$$C = \mathbf{1}^\top[A_z(1)a'(1) + B_z(1)b'(1)] + \frac{y'(1)}{z+\alpha} = 0, \tag{70}$$

hence $C = 0$ for all $x \in \overline{\Omega}$.
Thus we can rewrite system (67) as

$$\begin{cases} \rho\big[A_z(x)b'(x) + B_z(x)a'(x)\big] = 0, \\ \mathbf{1}^\top[A_z(x)a'(x) + B_z(x)b'(x)] = -\frac{y'(x)}{z+\alpha}. \end{cases} \tag{71}$$

It is now possible to augment $\hat{M}_z$ and $\hat{K}_z$ in order to make them quadratic. Adding the vector $\rho = [\rho_1, \rho_2, \dots, \rho_{n+1}]$ as another row in $\hat{M}_z$, and $[1\,1\,\dots\,1]^\top$ as an extra row in $\hat{K}_z$ gives a system for $a(x), b(x)$, given by

$$\begin{cases} K_z[A_z(x)a'(x) + B_z b'(x)] = -\dfrac{y'(x)}{z+\alpha}\begin{bmatrix}0\\0\\1\end{bmatrix}, & \text{(72a)} \\ M_z[B_z(x)a'(x) + A_z(x)b'(x)] = -\dfrac{y(x)}{z+\alpha}\begin{bmatrix}1\\1\\0\end{bmatrix}, & \text{(72b)} \end{cases}$$

with

$$\begin{aligned} [K_z]_{j,i} &:= \begin{cases} \dfrac{k_j(z)}{k_j(z)^2 - \rho_i(z)^2} & \forall i, j, \\ 1 & \forall i,\ j = N+1, \end{cases} \\ [M_z]_{j,i} &:= \begin{cases} \dfrac{\rho_i(z)}{k_j(z)^2 - \rho_i(z)^2} & \forall i, j, \\ \rho_i & \forall i,\ j = N+1. \end{cases} \end{aligned} \tag{73}$$

Before continuing we want to proof the invertability of the, now, square matrices K_z, M_z.

Lemma 10. *Suppose that $z \notin \varsigma$ and that the characteristic polynomial P_z has $2N+2$ different roots $\pm\rho_1, \dots, \pm\rho_{N+1}$, then the matrices K_z and M_z are invertible.*

Proof. See Appendix 7.2 □

We want to reformulate system (72a) and (72b) in order to get a representation of $a'(x), b'(x)$. To achieve that we first multiply $(A_z K_z)^{-1}$ with (72a), (remember: A_z, B_z are diagonal matrices and hence they follow the commutative rule as well as being invertible), and get

$$a'(x) = -(A_z(x)K_z)^{-1}\frac{y'(x)}{z+\alpha}\begin{bmatrix}0\\0\\1\end{bmatrix} - A_z^{-1}(x)B_z(x)b'(x). \tag{74}$$

Inserting (74) into (72b) to get $b'(x)$ delivers

$$M_z[B_z(x)\big[-(A_z(x)K_z)^{-1}\frac{y'(x)}{z+\alpha}\begin{bmatrix}0\\0\\1\end{bmatrix}-A_z^{-1}(x)B_z(x)b'(x)\big]+A_z(x)b'(x)] = -\frac{y(x)}{z+\alpha}\begin{bmatrix}1\\1\\0\end{bmatrix}, \tag{75}$$

multiplying with M_z^{-1} and separating $b'(x)$ gives

$$[A_z(x)-A_z^{-1}(x)B_z^2(x)]b'(x) = -M_z^{-1}\frac{y(x)}{z+\alpha}\begin{bmatrix}1\\1\\0\end{bmatrix}+B_z(x)(A_z(x)K_z)^{-1}\frac{y'(x)}{z+\alpha}\begin{bmatrix}0\\0\\1\end{bmatrix}, \tag{76}$$

multiplying both sides with $A_z(x)$ and exploiting that $A_z^2(x)-B_z^2(x)=\mathbf{1}$ gives

$$b'(x) = -A_z(x)M_z^{-1}\frac{y(x)}{z+\alpha}\begin{bmatrix}1\\1\\0\end{bmatrix}+B_z(x)K_z^{-1}\frac{y'(x)}{z+\alpha}\begin{bmatrix}0\\0\\1\end{bmatrix}. \tag{77}$$

Re-substituting (77) into (74) gives

$$\begin{aligned} a'(x) =& -(A_z(x)K_z)^{-1}\frac{y'(x)}{z+\alpha}\begin{bmatrix}0\\0\\1\end{bmatrix}+A_z^{-1}(x)B_z(x)\big[A_z(x)M_z^{-1}\frac{y(x)}{z+\alpha}\begin{bmatrix}1\\1\\0\end{bmatrix} \\ & +B_z(x)K_z^{-1}\frac{y'(x)}{z+\alpha}\begin{bmatrix}0\\0\\1\end{bmatrix}\big], \end{aligned} \tag{78}$$

grouping the terms containing K_z^{-1} together gives

$$a'(x) = -A_z^{-1}(x)[\mathbf{1}+B_z^2(x)]K_z^{-1}\frac{y'(x)}{z+\alpha}\begin{bmatrix}0\\0\\1\end{bmatrix}+B_z(x)M_z^{-1}\frac{y(x)}{z+\alpha}\begin{bmatrix}1\\1\\0\end{bmatrix}, \tag{79}$$

exploiting again $A_z^2(x)=\mathbf{1}+B_z^2(x)$ we get

$$a'(x) = -A_z(x)K_z^{-1}\frac{y'(x)}{z+\alpha}\begin{bmatrix}0\\0\\1\end{bmatrix}+B_z(x)M_z^{-1}\frac{y(x)}{z+\alpha}\begin{bmatrix}1\\1\\0\end{bmatrix}. \tag{80}$$

Recapitulating we define

$$aa(x) := -A_z(x)K_z^{-1}\frac{y'(x)}{z+\alpha}\begin{bmatrix}0\\0\\1\end{bmatrix} + B_z(x)M_z^{-1}\frac{y(x)}{z+\alpha}\begin{bmatrix}1\\1\\0\end{bmatrix}, \tag{81}$$

$$bb(x) := -A_z(x)M_z^{-1}\frac{y(x)}{z+\alpha}\begin{bmatrix}1\\1\\0\end{bmatrix} + B_z(x)K_z^{-1}\frac{y'(x)}{z+\alpha}\begin{bmatrix}0\\0\\1\end{bmatrix}, \tag{82}$$

and hence

$$a(x) = a_{0,z} + \frac{1}{2}\left(\int_{-1}^{x} aa(r)dr - \int_{x}^{1} aa(r)dr\right), \tag{83}$$

$$b(x) = b_{0,z} + \frac{1}{2}\left(\int_{-1}^{x} bb(r)dr - \int_{x}^{1} bb(r)dr\right). \tag{84}$$

We would like now to compute the exact form of both $a_{0,z}$ and $b_{0,z}$; to do this we finally need to focus on the boundary condition.
From (61) and (62) it is known that for the non-square matrices $\hat{S}_z^e$ and $\hat{S}_z^o$ as in (30), it holds that

$$\hat{S}_z^e a(1) + S_z^o b(1) = 0, \tag{85}$$

$$\hat{S}_z^e a(-1) - S_z^o b(-1) = 0. \tag{86}$$

As with the matrices $\hat{K}_z, \hat{M}_z$ we would like to augment $\hat{S}_z^e$ and $\hat{S}_z^o$ into square matrices; for this case, similar as in the homogeneous situation, the Neumann boundary condition comes to aid. We will consider

$$D\frac{dq}{dx}(x)\bigg|_{x=\pm 1} = 0. \tag{87}$$

Inserting the Ansatz $q(x)$ in equation (87) and dividing both sides by $D \neq 0$ gives

$$\begin{aligned} 0 = \frac{y'(x)}{z+\alpha} + \sum_{i=1}^{N+1} \big[& a_i'(x)\cosh(\rho_i(z)x) + \rho_i a_i(x)\sinh(\rho_i(z)x) \\ & + b_i'(x)\sinh(\rho_i(z)x) + \rho_i b_i(x)\cosh(\rho_i(z)x)\big]\bigg|_{x=\pm 1}. \end{aligned} \tag{88}$$

Rewriting it into matrix-vector form as done earlier gives

$$0 = \frac{y'(\pm 1)}{z+\alpha} + \rho[B_z(\pm 1)a(\pm 1) + A_z(\pm 1)b(\pm 1)] + \mathbf{1}^\top[A_z(\pm 1)a'(\pm 1) + B_z(\pm 1)b'(\pm 1)]. \tag{89}$$

Again, because both $a, b, y \in Y := \{y \in C^2(\overline{\Omega}) | y'(\pm 1) = 0)\}$, it holds that

$$0 = +\rho[B_z(\pm 1)a(\pm 1) + A_z(\pm 1)b(\pm 1)], \tag{90}$$

and because $A_z(-1) = A_z(1)$ and $B_z(-1) = -B_z(1)$ it follows that

$$0 = \rho[B_z(1)a(1) + A_z(1)b(1)], \tag{91}$$
$$0 = \rho[-B_z(1)a(-1) + A_z(1)b(-1)]. \tag{92}$$

This shows that the coefficients $a, b \in Y$ need to satisfy following systems on the boundary

$$\begin{cases} \hat{S}_z^e a(1) + \hat{S}_z^o b(1) = 0, \\ \rho[B_z(1)a(1) + A_z(1)b(1)] = 0, \end{cases} \tag{93}$$

and

$$\begin{cases} \hat{S}_z^e a(-1) - \hat{S}_z^o b(-1) = 0, \\ \rho[-B_z(1)a(-1) + A_z(1)b(-1)] = 0. \end{cases} \tag{94}$$

Again we modify $\hat{S}_z^e$ and $\hat{S}_z^o$ such as to make them quadratic. We hence define

$$S_z^e := \begin{bmatrix} \hat{S}_z^e \\ [\rho_i \sinh(\rho_i)]_i \end{bmatrix}, \tag{95}$$

$$S_z^o := \begin{bmatrix} \hat{S}_z^o \\ [\rho_i \cosh(\rho_i)]_i \end{bmatrix}, \tag{96}$$

getting

$$\mathrm{S}_\mathrm{z}^\mathrm{e}\, a(1) + \mathrm{S}_\mathrm{z}^\mathrm{o}\, b(1) = 0, \tag{97}$$

and

$$\mathrm{S}_\mathrm{z}^\mathrm{e}\, a(-1) - \mathrm{S}_\mathrm{z}^\mathrm{o}\, b(-1) = 0. \tag{98}$$

By substituting (83) and (84) into (97) and (98), it is now possible to determine $a_{0,z}$ and $b_{0,z}$.
It follows that

$$\mathrm{S}_\mathrm{z}^\mathrm{e}\, a_{0,z} + \frac{1}{2}\mathrm{S}_\mathrm{z}^\mathrm{e}\left(\int_{-1}^{1} aa(r)dr\right) + \mathrm{S}_\mathrm{z}^\mathrm{o}\, b_{0,z} + \frac{1}{2}\mathrm{S}_\mathrm{z}^\mathrm{o}\left(\int_{-1}^{1} bb(r)dr\right) = 0, \tag{99}$$

$$\mathrm{S}_\mathrm{z}^\mathrm{e}\, a_{0,z} - \frac{1}{2}\mathrm{S}_\mathrm{z}^\mathrm{e}\left(\int_{-1}^{1} aa(r)dr\right) - \mathrm{S}_\mathrm{z}^\mathrm{o}\, b_{0,z} + \frac{1}{2}\mathrm{S}_\mathrm{z}^\mathrm{o}\left(\int_{-1}^{1} bb(r)dr\right) = 0. \tag{100}$$

Next, we respectively, add (99) to (100) or subtract (99) to (100) to obtain

$$2\,\mathrm{S}_\mathrm{z}^\mathrm{e}\, a_{0,z} + \mathrm{S}_\mathrm{z}^\mathrm{o}\left(\int_{-1}^{1} bb(r)dr\right) = 0, \tag{101}$$

$$\mathrm{S}_\mathrm{z}^\mathrm{e}\left(\int_{-1}^{1} aa(r)dr\right) + 2\,\mathrm{S}_\mathrm{z}^\mathrm{o}\, b_{0,z} = 0, \tag{102}$$

respectively. From the above two equalities we finally get

$$a_{0,z} = -\frac{1}{2}\,\mathrm{S}_{\mathrm{z}}^{\mathrm{e}-1}\,\mathrm{S}_{\mathrm{z}}^{\mathrm{o}}\left(\int_{-1}^{1} bb(r)dr\right), \tag{103}$$

$$b_{0,z} = -\frac{1}{2}\,\mathrm{S}_{\mathrm{z}}^{\mathrm{o}-1}\,\mathrm{S}_{\mathrm{z}}^{\mathrm{e}}\left(\int_{-1}^{1} aa(r)dr\right). \tag{104}$$

This yields

$$a(x) = -\frac{1}{2}\,\mathrm{S}_{\mathrm{z}}^{\mathrm{e}-1}\,\mathrm{S}_{\mathrm{z}}^{\mathrm{o}}\left(\int_{-1}^{1} bb(r)dr\right) + \frac{1}{2}\left(\int_{-1}^{x} aa(r)dr - \int_{x}^{1} aa(r)dr\right), \tag{105}$$

$$b(x) = -\frac{1}{2}\,\mathrm{S}_{\mathrm{z}}^{\mathrm{o}-1}\,\mathrm{S}_{\mathrm{z}}^{\mathrm{e}}\left(\int_{-1}^{1} aa(r)dr\right) + \frac{1}{2}\left(\int_{-1}^{x} bb(r)dr - \int_{x}^{1} bb(r)dr\right). \tag{106}$$

with $aa(x), bb(x)$ as in (81) and (82).
For completeness we have to check if the choices for $a(x), b(x)$, with these $a_{0,z}, b_{0,z}$ really solve systems (72a) and (72b). It comprises nothing else than substituting $a(x), b(x)$ into the system and can be found in the Appendix.

6 Numerical Analysis

It is possible to numerically analyse an approximated solution of the delayed diffusion neural field equation as done similarly in [2] and [1]. To do this we have to discretize $\overline{\Omega} = [-1, 1]$ and by doing this we get a system of equations with $m+1$ delays. Some derivation and a deeper inside into the discretization process are explained in [5] and [8]. The system (NFE) discretized has following form

$$\frac{dV_i}{dt}(t) = -\alpha V_i(t) - \frac{D}{h^2}MV + h\sum_{j=1}^{m+1}\xi_j \hat{J}(|i-j|h) \times S(V_j(t-\tau_0-|i-j|h)). \tag{107}$$

for $i = 1, \ldots, m+1$ and

$$\xi_j = \begin{cases} \frac{1}{2} & \text{if } j \in \{1, m+1\}, \\ 1 & \text{otherwise,} \end{cases}$$

and $h = \frac{2}{m}$ the discretization of $\overline{\Omega}$ in m equally long segments. M is a tridiagonal matrix with ones on the lower and upper diagonal, and -2 on the main diagonal, with the exclusion of $M_{11} = M_{nn} = -1$. The diffusive part has been discretized through a centred finite difference method. We take $N = 2$ and $\hat{J} : \mathcal{R} \to \mathcal{R}$ as in (10); more precisely we will use

$$J_1(x) = 12.5 \cdot e^{-2|x|} - 10 \cdot e^{-|x|}, \tag{108}$$

$$J_2(x) = 3 \cdot e^{-0.5|x|} - 5.5 \cdot e^{-|x|}, \tag{109}$$

where J_1 is a Mexican-hat type function and J_2 is an inverted Mexican-hat type function (Figure 1). This section will be structured as following: first we will

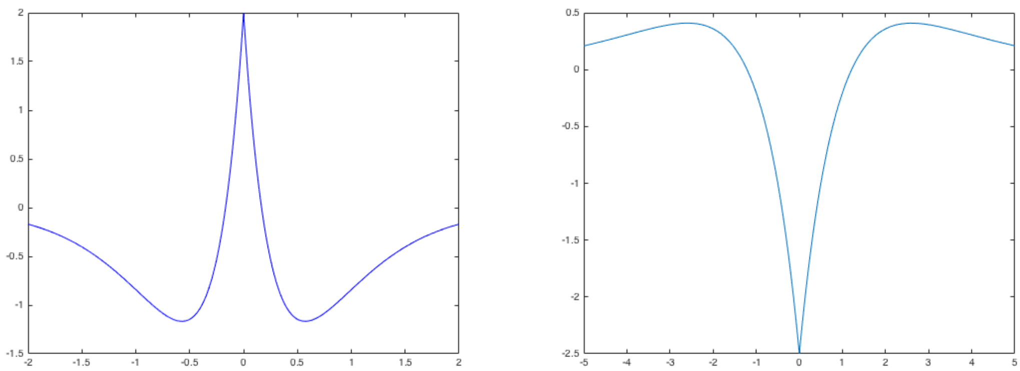

Fig. 1. Connectivity functions J_1 and J_2, respectively.

show how for $D \to 0$, the "diffusive spectrum" converges towards the non-diffusive spectrum computed in [2] and [1]. After that, we will proceed with a bifurcation analysis for both J_1, J_2. We will show the presence of a fold bifurcation as well as Hopf bifurcation. Finally we will concentrate on co-dimension 2 bifurcations by finding a Pitchfork-Hopf bifurcation for J_1.

6.1 Convergence of Spectrum

It is in our interest to understand the influence of the diffusion term D on the spectrum of the problem. We will show that for $D \to 0$ the spectrum converges towards the spectrum of the non diffusive problem. We will however run into some difficulties for small D and we will try to explain the origin of this. First we will check if the same convergences applies to the Hopf bifurcation of [1], for J_2; next we will study the Pitchfork-Hopf bifurcation occurring for J_1 in [2] . In [1] a

Parameter	α	$\hat{c}_1$	$\hat{c}_2$	μ_1	μ_2	r	τ_0
J_1	1	12.5	-10	2	1	2.5169	2.5939
J_2	1	3	-5.5	0.5	1	4.2202	1

Table 1: Parameters computed in [2] and [1] for which in the non-diffusive case ($D = 0$) a Pitchfork-Hopf and a Hopf Bifurcation appear, respectively.

Hopf-Bifurcation was found for connectivity J_2 and parameters as in Table 1. We calculated analytically the spectrum and confirmed the results in [1], by finding the Hopf bifurcation, as shown in Figure 2.

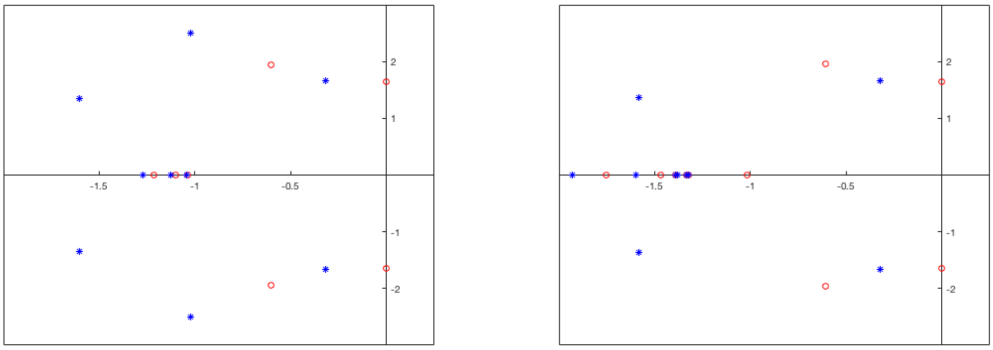

Fig. 2. Left: spectrum for connectivity J_2 and parameters as in Table 1. **Right:** spectrum computed analytically for low diffusive case $D = 0.005$. (*Even and odd eigenvalues are shown as red circles and blue stars, respectively.*)

.

Figure 2 confirms that the discretisation (107) is valid and it also confirms the presence of an "accumulation region" near the point $-\alpha$, (for $\alpha = 2$ the accumulation region is near -2). We notice that the position of the eigenvalues which are not on the x-axis has varied little from the non-diffusive case; however the accumulation region has been spread more and pushed to the left.

In [2] a Pitchfork-Hopf bifurcation was found for parameters as in Table 1 and connectivity J_1, without diffusion ($D = 0$). By keeping the parameters unchanged but varying the diffusion coefficient D, it is easy to see that the eigenvalues converge towards the Pitchfork-Hopf bifurcation for $D \to 0$, (See Figure 3). Analytically it was possible to compute the eigenvalues up to $D = 0.005$; for lower values the error increases dramatically due to the very small third root of the characteristic polynomial. With the aid of a numerical bifurcation package for Matlab named `Biftool` [10], we were able to show the convergence for even lower values $D < 0.0001$.
In Figure 3 (b), the nearly critical eigenvalue z_1 and nearly critical z_2 are

$$z_1 = -0.0069 \pm 0i, \tag{110}$$

$$z_2 = -0.0001 \pm 0.6879i. \tag{111}$$

The fact that both z_1, z_2 are nearly the same as λ_1, λ_2 in [2] furthermore confirms the convergence of the spectrum.

6.2 Fold, Hopf and Pitchfork-Hopf bifurcations

Before we start with the actual spectrum analysis some minor remarks are necessary:

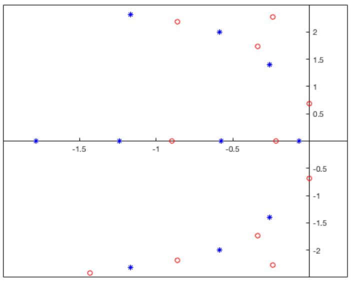

(a) $D = 0.1$

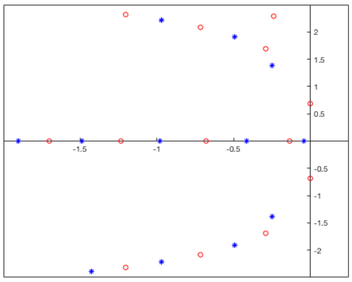

(b) $D = 0.05$

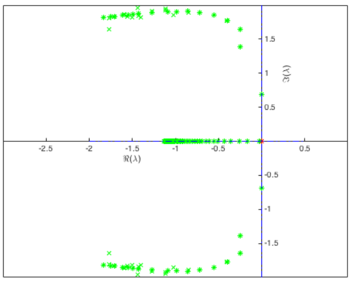

(c) $D = 0.0001$. Computed through `Biftool`

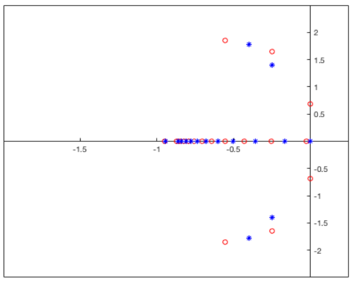

(d) $D = 0$

Fig. 3. Spectra for connectivity J_1, parameters as in Table 1 and various D. Unfortunately `Biftool` does not recognize which eigenvalue is "even" and which "odd", hence the difference in colour from the other figures.(*Even and odd eigenvalues are shown as red circles and blue stars, respectively.*)

Remark 11.

- *An increase in the value of r causes a movement of all eigenvalues towards the right half plane.*

- *A change in the value of D affects mostly only the eigenvalues on the x-axis*

- *τ_0 instead affects the eigenvalues that are not on the axis.*

6.2.1 Fold Bifurcation

α	$\hat{c}_1$	$\hat{c}_2$	μ_1	μ_2	r	τ_0	D
1	12.5	-10	2	1	3.28	1	0.08

Table 2: Parameters for which a fold-bifurcation appears.

For parameters as in Table 2 we notice the presence of a fold-bifurcation equivalent to a zero "odd" eigenvalue. We will not study this bifurcation further.

6.2.2 Hopf Bifurcation

We are free of using whatever parameters as our free bifurcation parameters. First we use only τ and r with the other parameters and especially D fixed like in Table 3. We get the expected Hopf branches as depicted in Figure 4.
If however we fix r and the other values and use τ and D as bifurcation parameters

	α	$\hat{c}_1$	$\hat{c}_2$	μ_1	μ_2	r	τ_0	D
J_1	1	12.5	-10	2	1	2.5169	2.5517	1
J_2	1	3	-5.5	0.5	1	3.559	1.5	0.5

Table 3: Parameters for which a Hopf-bifurcation appears, with τ and r bifurcation parameters.

we get also Hopf branches as depicted in Figure 5, where the spectrum was

	α	$\hat{c}_1$	$\hat{c}_2$	μ_1	μ_2	r	τ_0	D
$\tilde{J}_1$	1	12.5	-10	2	1	3.28	0.7532	0.7
$\tilde{J}_2$	1	3	-5.5	0.5	1	4.2202	1.0655	0.7

Table 4: Parameters for which a Hopf-bifurcation appears, with D and τ bifurcation parameters.

computed with parameters having values as in Table 4. We see that in all the

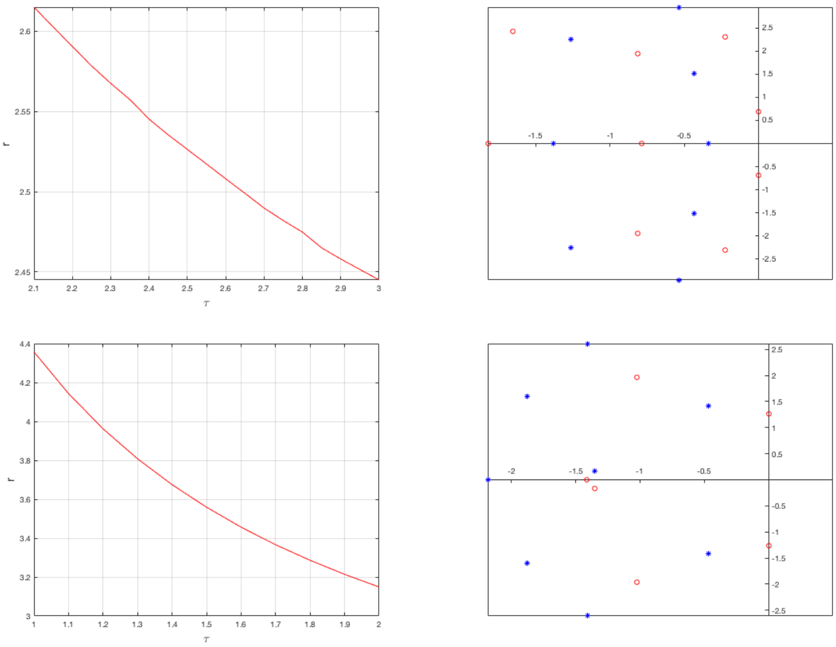

Fig. 4. Left: Hopf curves on the background state for connectivity J_1 and J_2, respectively. **Right:** eigenvalues for parameters as in Table 3.(*Even and odd eigenvalues are shown as red circles and blue stars, respectively.*)

spectra the purely imaginary eigenvalues are "even". We will hence calculate the various coefficients a_1, a_2, a_3; to do this we will take the values of J_1 in Table 3, where the free parameters where τ and r, and the values of $\tilde{J}_2$ in Table 4. We get

$$\pm\lambda_1 = 0.6958i, \qquad \pm\lambda_2 = 1.5850i, \tag{112}$$

respectively. Computations with λ_1 then gives for connectivity J_1,

$$\begin{aligned} \rho_1^{(1)} &= 2.4463 - 0.1750i, & \qquad & a_1^{(1)} &= -0.0319, \\ \rho_2^{(1)} &= 0.1380 - 0.6938i, & \text{and} \quad & a_2^{(1)} &= -0.8351 - 0.5437i, \\ \rho_3^{(1)} &= 1.6548 + 1.7882i, & & a_3^{(1)} &= -0.0589 + 0.0499i, \end{aligned} \tag{113}$$

and for $\tilde{J}_2$ and λ_2 we get

$$\begin{aligned} \rho_1^{(2)} &= 0.1905 + 1.8950i, & \qquad & a_1^{(2)} &= -0.1557, \\ \rho_2^{(2)} &= 2.0529 + 1.6136i, & \text{and} \quad & a_2^{(2)} &= -0.0139 + 0.0530i, \\ \rho_3^{(2)} &= 0.2414 - 0.6783i, & & a_3^{(2)} &= -0.6382 - 0.7520i. \end{aligned} \tag{114}$$

Having computed the coefficients for both connectivity, and due to the same parity condition of the critical eigenvalue, it is possible to write down the general form of

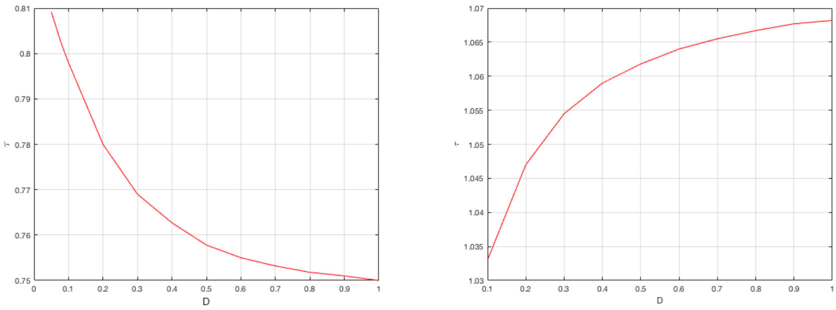

Fig. 5. **Left:** Hopf curve on the background state for connectivity $\tilde{J}_1$. **Right:** Hopf curve on the background state for $\tilde{J}_2$, respectively.

the complex eigenfunction of both connectivities as

$$\psi_{\lambda_j}(t,x)) := e^{\lambda_j t}\big(a_1^{(j)}\cosh(\rho_1^{(j)}x) + a_2^{(j)}\cosh(\rho_2^{(j)}x) + a_3^{(j)}\cosh(\rho_3^{(j)}x)\big), \tag{115}$$

for $j = \{1,2\}$ and $t \in [-h,0]$. The two different eigenfunction can be seen in Figure 7

6.2.3 Pitchfork-Hopf Bifurcation

Most interesting is the situation of a co-dimension 2 bifurcation. Similarly to [2] we will find a Pitchfork-Hopf bifurcation for connectivity J_1.

α	$\hat{c}_1$	$\hat{c}_2$	μ_1	μ_2	r	τ_0	D
1	12.5	-10	2	1	3.28	0.802	0.08

Table 5: Parameters for which a Pitchfork Hopf-bifurcation appears.

Solving (26) for values as in Table 5 delivers an "odd" zero eigenvalue and two "even" purely imaginary eigenvalues

$$\lambda_1 = 0, \qquad \pm\lambda_2 = 1.2091i. \tag{116}$$

Continuation of the bifurcation curves are shown in Figure 8, the corresponding eigenfunctions have the form

$$\psi_1(x,t) = b_1\sinh(\rho_1 x) + b_2\sinh(\rho_2 x) + b_3\sinh(\rho_3 x), \tag{117}$$

$$\psi_2(x,t) = e^{\lambda_2 t}\big(a_1\cosh(\rho_1^{(2)}x) + a_2\cosh(\rho_2^{(2)}x) + a_3\cosh(\rho_3^{(2)}x)\big). \tag{118}$$

(119)

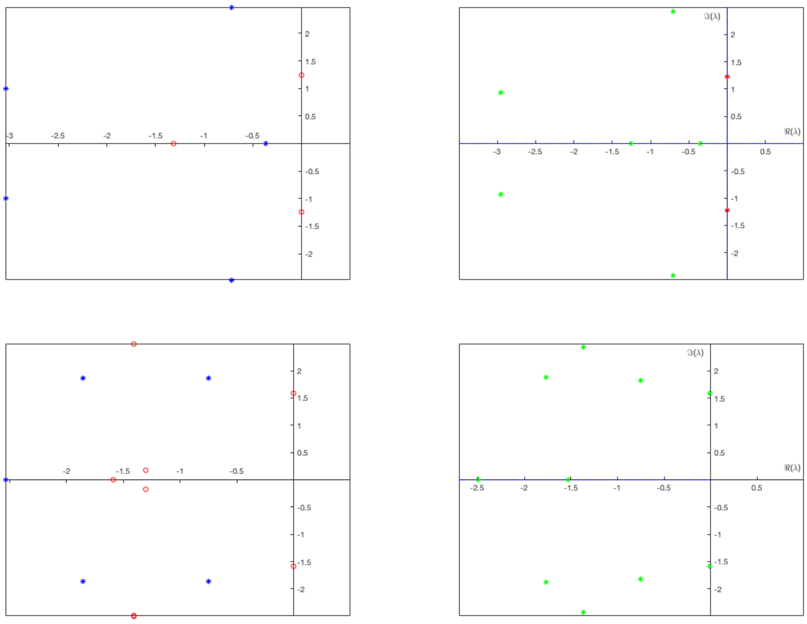

Fig. 6. Left: Spectrum computed analytically for parameters as in Table 4. (*Even and odd eigenvalues are shown as red circles and blue stars, respectively.*) **Right:** Spectrum computed through `Biftool`. (*Stable and unstable eigenvalues are shown in red and blue, respectively*).

A quick computation gives for $\lambda_1 = 0$,

$$\begin{aligned} \rho_1 &= 5.1902, & & & b_1 &= -0.0018 - 0.0035i, \\ \rho_2 &= 2.7784i, & &\text{and} & b_2 &= -0.7053 + 0.3696i, \\ \rho_3 &= -1.3111i, & & & b_3 &= 0.5358 - 0.2808i, \end{aligned} \tag{120}$$

and for $\lambda_2 = 1.2091i$,

$$\begin{aligned} \rho_1^{(2)} &= 4.9760 + 0.5701i, & & & a_1 &= -0.0010 + 0.0022i, \\ \rho_2^{(2)} &= 0.2638 - 0.8660i, & &\text{and} & a_2 &= -0.8695 - 0.4911i, \\ \rho_3^{(2)} &= 2.2665 + 3.7837i, & & & a_3 &= 0.04931. \end{aligned} \tag{121}$$

The eigenfunction can be seen in Figure 9. It is possible to solve the discretization problem, as done before, using a classical DDE Matlab solver like `dde23`. This delay differential equation solver is derived from the more known ODE solver `ode23`. The solver `dde23` wa used with default relative tolerance of 1e-3 and an absolute tolerance of 1e-6. The input variables were the history function (initial condition), the lags, the delays and of course the discretized system.

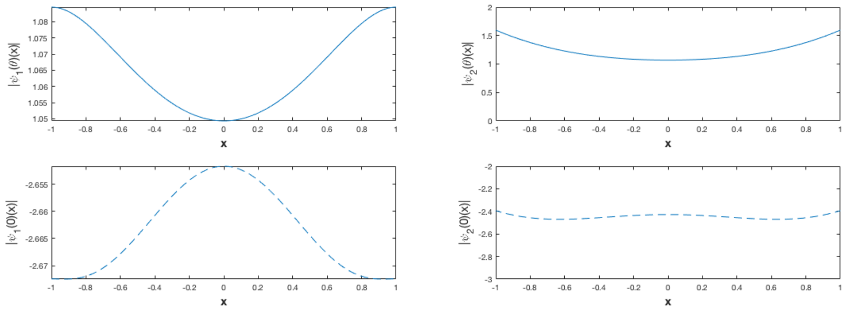

Fig. 7. Left complex-valued eigenfunction (115) for connectivity J_1 as in Table 3. **Right:** complex-valued eigenfunction (115) for connectivity $\tilde{J}_2$ as in Table 4.

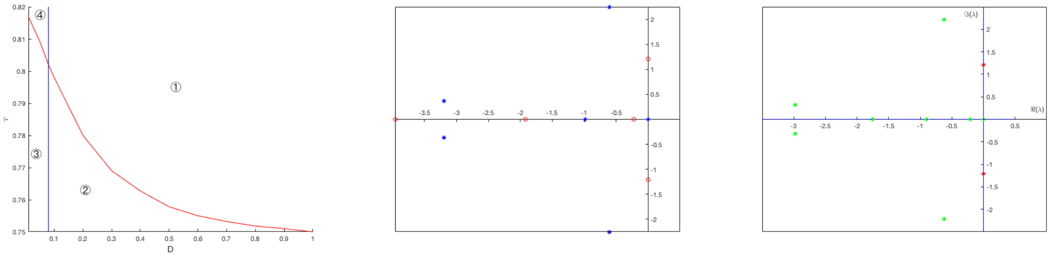

Fig. 8. Left: Pitchfork-Hopf curves for background state. **Middle:** analytically computed eigenvalues for parameters as in Table 5.(*Even and odd eigenvalues are shown as red circles and blue stars, respectively*). **Right:** Spectrum computed through `Biftool`. (*Stable and unstable eigenvalues are shown in red and blue, respectively*).

We chose as initial conditions following functions

$$V(x,t) = 0.05 \cdot (0.99 \cdot \psi_{\lambda_1}(0) + 0.01 \cdot \psi_{\lambda_2}(0)), \tag{122}$$

$$V(x,t) = 0.05 \cdot (0.01 \cdot \psi_{\lambda_1}(0) + 0.99 \cdot \psi_{\lambda_2}(0)), \tag{123}$$

with $t \in [-(\tau_0 + 2), 0]$. We will see the behaviour of the solution for the various regimes shown in Figure 8. We first chose a time interval of $[0, 300]$ however after having run the code we realize that in some occasions more time was needed for the solution to stabilize, hence we ultimately chose different time intervals for different regions; The discretization was $m = 50$.

In region 1 we see that all solutions decay to zero for initial condition (122) while for initial condition (123) the only stable solution is a periodic oscillating solution (Figure 10). When passing from region 1 to region 2 we cross the Hopf-curve of Figure 8; the solution for (122) remains similar to the one of region 1, except that the solution decays relatively faster. For (123) instead it is possible to see how the periodic solutions slowly decays towards zero, with the firing rates becoming weaker

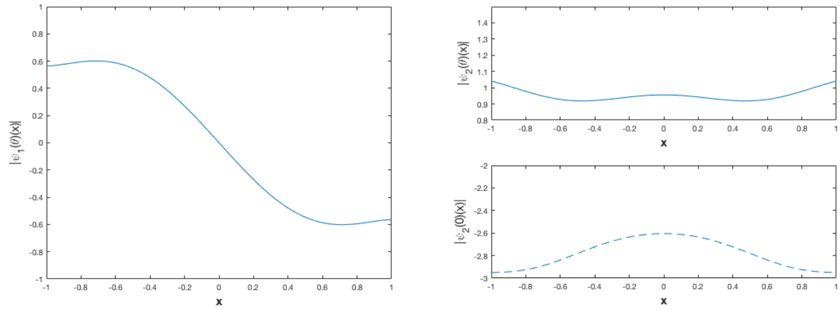

Fig. 9. Left: real-valued eigenfunction (117) for zero eigenvalue λ_1. **Right:** complex-valued eigenfunction (118) for imaginary eigenvalue λ_2.

(Figure 11). More interesting is the crossing of the fold-curve seen in Figure 12; here for the initial condition (122) we notice bi-stability: a stable stationary and a periodic solution appear. Interestingly enough the periodic solution for the second initial condition (123) appears to decay for increasing time, while for the other initial conditions the solution increases in strength. The final region 4 is similar to region 3 and is also characterized by bi-stability, however here for initial condition (123) the periodic solution stabilizes itself instead of decaying (Figure 13).

6.3 Influence of diffusion on spectrum

The addition of diffusion on NFE appears not to have any influence on the stability of the solution; however it does influence the spectrum in quite some other way. Take Figure 6 as an example: we clearly notice how the diffusion spreads the eigenvalues on the x-axis making the accumulation point near α disappear. The spread of the eigenvalue is however not only viewable in on the axis; if for example we take Figure 2 we notice how the eigenvalues increase in height (respective to the y-axis) when the diffusion coefficient is added.

None of the bifurcations disappear with addition of diffusion and both Hopf and Pitchfork-Hopf bifurcations can be found also with diffusion. When analysing however the solution through `DDE23`, as done above, we notice how in region 2, the solution needs more time than in the other regions to converge towards a stable state. It is however problematic to work with low values of D, as shortly commented before. For values of D smaller than 10^{-4} it becomes impossible to calculate analytically the eigenvalues; we encountered, for example, conditions number up to 10^{21} for the matrices S^e and S^o. The characteristic polynomial converges for $D \to 0$ towards a polynomial of one lower order, and hence one of

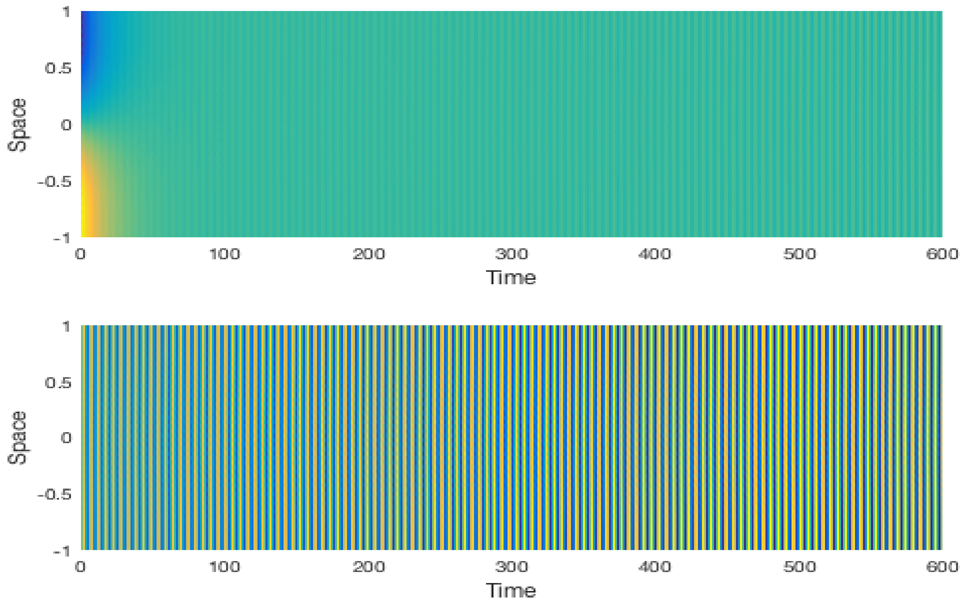

Fig. 10. Simulation of region 1 with $D = 0.15$ and $\tau_0 = 0.802$. The top and the bottom panels correspond to initial conditions (122) with a time interval of $[0, 300]$ and (123) with a time interval of $[0, 1000]$, respectively.

the roots converges towards 0, destabilizing the whole calculations done in this thesis; hence if working with low values of D it is necessary to use some numerical analysis package like, in our case, `Biftool`. In both figure 6 and 8 we notice how the eigenvalues computed analytically using the system (39) and equation (40), coincide with the one computed numerically through `Biftool`.

7 Discussion

This paper has studied the behaviour of one dimensional delay neural fields equation with diffusion.
We have shown how the computation of the spectrum changes once diffusion is added to the equation and how the symmetry arguments brought forward by Dijkstra in [2] can still be applied to this new situation.
Further we have shown how the analytically computed eigenvalues coincide with the numerically computed eigenvalues, using `Biftool`.
As done in many previous works an odd firing rate has been used, mainly because it is handy when working with symmetric arguments; there is however no biological reason to assume an odd parity of the firing rate, but it is common use to assume

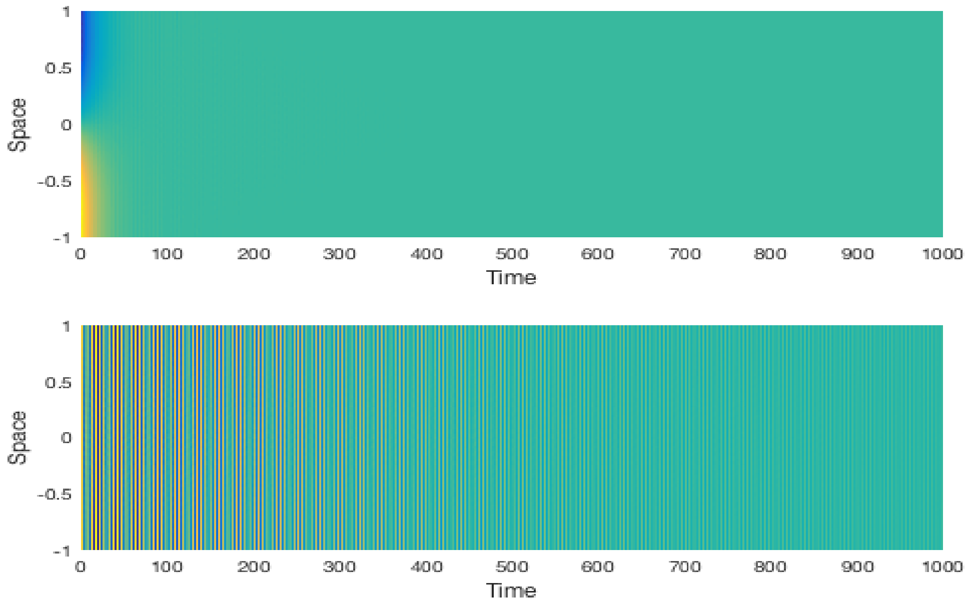

Fig. 11. Simulation of region 2 with $D = 0.15$ and $\tau_0 = 0.76$, both on a time interval of $[0, 1000]$. The top and the bottom panels correspond to initial conditions (122) and (123), respectively.

it. This was not the only assumption made in this paper; as mentioned in section 5.1, we made a big assumption when splitting (60c) into the system (66). Also here the mathematical assumption is (still) not backed up by biological reasoning and this should be extensively studied in future works.
Furthermore it has been shown how the addition of diffusion in the (NFE) does not change the type of bifurcation that appear and neither their stability. However it has of course an effect on the spectrum, it mostly "stretches" it. The accumulation area present on the x-axis of the Pitchfork-Hopf bifurcation in [1] is dispersed. Also, when analysing the behaviour of the solution we saw how because of the diffusion parameter more time is needed for the solutions to stabilize.
Again, as in [1] and [2] multi-stability of the solution has been observed. This means that the addition of an external input $I(x, t)$ would change permanently the dynamics of the solution; in many paper this external input has been taken into consideration and it would for sure be interesting to analyse in combination with diffusion. In our case, without the input factor we saw how a solution can switch from a stable stationary solution to a large scale oscillation, usually, biologically, attributed to an epileptic seizure [15].

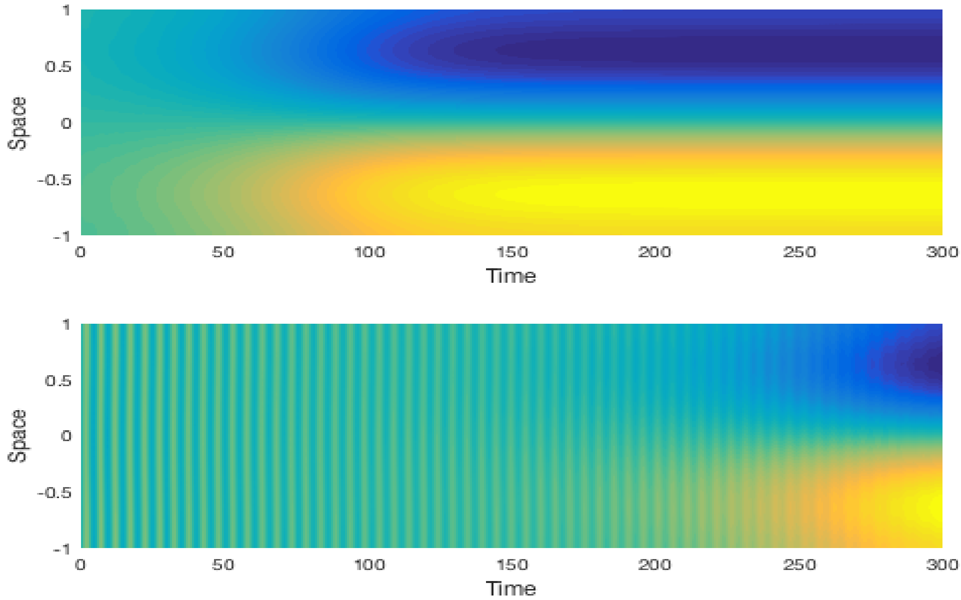

Fig. 12. Simulation of region 3 with $D = 0.05$ and $\tau_0 = 0.76$, both on a time interval of $[0, 300]$. The top and the bottom panels correspond to initial conditions (122) and (123), respectively.

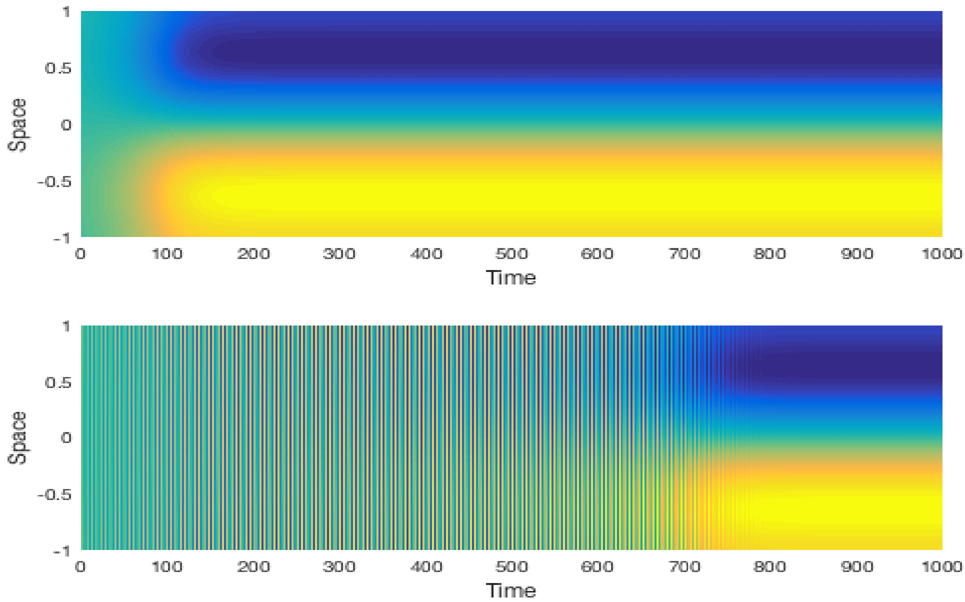

Fig. 13. Simulation of region 4 and $D = 0.05$ and $\tau_0 = 0.9$. The top and the bottom panels correspond to initial conditions (122) and (123), respectively.

8 Appendix

8.1 Correctness of $a(x), b(x)$

We want to show that

$$a(x) = a_{0,z} + \frac{1}{2}\left(\int_{-1}^{x} aa(r)dr - \int_{x}^{1} aa(r)dr\right), \tag{124}$$

$$b(x) = b_{0,z} + \frac{1}{2}\left(\int_{-1}^{x} bb(r)dr - \int_{x}^{1} bb(r)dr\right), \tag{125}$$

with

$$a_{0,z} = -\frac{1}{2}\,\mathrm{S}_{\mathrm{z}}^{\mathrm{e}-1}\,\mathrm{S}_{\mathrm{z}}^{\mathrm{o}}\left(\int_{-1}^{1} bb(r)dr\right), \tag{126}$$

$$b_{0,z} = -\frac{1}{2}\,\mathrm{S}_{\mathrm{z}}^{\mathrm{o}-1}\,\mathrm{S}_{\mathrm{z}}^{\mathrm{e}}\left(\int_{-1}^{1} aa(r)dr\right), \tag{127}$$

actually do solve the resolvent equation (55). We hence need to plug $a(x), b(x)$ in the systems (72b, 72a); these two system however have $aa(x), bb(x)$ as arguments. From (81) we know that

$$aa(x) = -A_z(x)K_z^{-1}\frac{y'(x)}{z+\alpha}\begin{bmatrix}0\\0\\1\end{bmatrix} + B_z(x)M_z^{-1}\frac{y(x)}{z+\alpha}\begin{bmatrix}1\\1\\0\end{bmatrix}, \tag{128}$$

$$b'(x) = -A_z(x)M_z^{-1}\frac{y(x)}{z+\alpha}\begin{bmatrix}1\\1\\0\end{bmatrix} + B_z(x)K_z^{-1}\frac{y'(x)}{z+\alpha}\begin{bmatrix}0\\0\\1\end{bmatrix}. \tag{129}$$

Plugging them into (72a) gives

$$\begin{aligned} &K_z[A_z(x)[-A_z(x)K_z^{-1}\frac{y'(x)}{z+\alpha}\begin{bmatrix}0\\0\\1\end{bmatrix} + B_z(x)M_z^{-1}\frac{y(x)}{z+\alpha}\begin{bmatrix}1\\1\\0\end{bmatrix}] \\ &- B_z(x)[A_z(x)M_z^{-1}\frac{y(x)}{z+\alpha}\begin{bmatrix}1\\1\\0\end{bmatrix} - B_z(x)K_z^{-1}\frac{y'(x)}{z+\alpha}\begin{bmatrix}0\\0\\1\end{bmatrix}]] = \begin{bmatrix}0\cdot\mathbf{1}\\ -\frac{y'(x)}{z+\alpha}\end{bmatrix}. \end{aligned} \tag{130}$$

Expanding the above form gives

$$
\begin{aligned}
&- A_z^2(x) - \frac{y'(x)}{z+\alpha}\begin{bmatrix}0\\0\\1\end{bmatrix} K_z A_z(x) B_z(x) M_z^{-1} \frac{y(x)}{z+\alpha}\begin{bmatrix}1\\1\\0\end{bmatrix}] \\
&- K_z B_z(x) A_z(x) M_z^{-1} \frac{y(x)}{z+\alpha}\begin{bmatrix}1\\1\\0\end{bmatrix} + B_z^2(x)\frac{y'(x)}{z+\alpha}\begin{bmatrix}0\\0\\1\end{bmatrix}]] = -\frac{y'(x)}{z+\alpha}\begin{bmatrix}0\\0\\1\end{bmatrix}.
\end{aligned} \tag{131}
$$

Hence,

$$
-\left(A_z^2(x) - B_z^2(x)\right)\frac{y'(x)}{z+\alpha}\begin{bmatrix}0\\0\\1\end{bmatrix} = -\frac{y'(x)}{z+\alpha}\begin{bmatrix}0\\0\\1\end{bmatrix}, \tag{132}
$$

and exploiting again that $A_z^2(x) - B_z^2(x) = \mathbf{1}$ gives

$$
-\frac{y'(x)}{z+\alpha}\begin{bmatrix}0\\0\\1\end{bmatrix} = -\frac{y'(x)}{z+\alpha}\begin{bmatrix}0\\0\\1\end{bmatrix} \tag{133}
$$

Analogously, plugging (81) into (72b) gives

$$
\begin{aligned}
&M_z[-B_z(x)\big(A_z(x) K_z^{-1}\frac{y'(x)}{z+\alpha}\begin{bmatrix}0\\0\\1\end{bmatrix} - B_z(x) M_z^{-1}\begin{bmatrix}-\frac{y(x)}{z+\alpha}\mathbf{1}\\0\end{bmatrix}\big) \\
&- A_z(x)\big(A_z(x) M_z^{-1}\frac{y(x)}{z+\alpha}\begin{bmatrix}1\\1\\0\end{bmatrix} + B_z(x) K_z^{-1}\frac{y'(x)}{z+\alpha}\begin{bmatrix}0\\0\\1\end{bmatrix}\big)] = -\frac{y(x)}{z+\alpha}\begin{bmatrix}1\\1\\0\end{bmatrix},
\end{aligned} \tag{134}
$$

expansion gives

$$
\begin{aligned}
&+ M_z B_z(x) A_z(x) K_z^{-1}\frac{y'(x)}{z+\alpha}\begin{bmatrix}0\\0\\1\end{bmatrix} + B_z^2(x)\frac{y(x)}{z+\alpha}\begin{bmatrix}1\\1\\0\end{bmatrix} \\
&- A_z^2(x)\frac{y(x)}{z+\alpha}\begin{bmatrix}1\\1\\0\end{bmatrix} - M_z A_z(x) B_z(x) K_z^{-1}\frac{y'(x)}{z+\alpha}\begin{bmatrix}0\\0\\1\end{bmatrix} = -\frac{y(x)}{z+\alpha}\begin{bmatrix}1\\1\\0\end{bmatrix},
\end{aligned} \tag{135}
$$

and using $A_z^2(x) - B_z^2(x) = \mathbf{1}$ gives

$$
\frac{y(x)}{z+\alpha}\begin{bmatrix}1\\1\\0\end{bmatrix} = \frac{y(x)}{z+\alpha}\begin{bmatrix}1\\1\\0\end{bmatrix}. \tag{136}
$$

This shows that the solutions $a(x), b(x)$ computed in (105,106) solve the systems (72a,72b). We will quickly show now that also the boundary condition is satisfied for the chosen values of $a(x), b(x)$. The proceeding is the same: we plug the functions into the boundary systems (97,98). We begin with (97):

$$\begin{aligned} \mathrm{S}_z^e\, a(1) + \mathrm{S}_z^o\, b(1) = &- \frac{1}{2}\, \mathrm{S}_z^o \int_{-1}^{1} bb(r)dr + \frac{1}{2}\, \mathrm{S}_z^e \int_{-1}^{1} aa(r)dr - \frac{1}{2}\, \mathrm{S}_z^e \int_{-1}^{1} aa(r)dr \\ &+ \frac{1}{2}\, \mathrm{S}_z^o \int_{-1}^{1} bb(r)dr = 0. \end{aligned} \tag{137}$$

For (98), we instead get

$$\begin{aligned} \mathrm{S}_z^e\, a(-1) - \mathrm{S}_z^o\, b(-1) = &- \frac{1}{2}\, \mathrm{S}_z^o \int_{-1}^{1} bb(r)dr - \frac{1}{2}\, \mathrm{S}_z^e \int_{-1}^{1} aa(r)dr + \frac{1}{2}\, \mathrm{S}_z^e \int_{-1}^{1} aa(r)dr \\ &+ \frac{1}{2}\, \mathrm{S}_z^o \int_{-1}^{1} bb(r)dr = 0. \end{aligned} \tag{138}$$

We have shown hence, that for all $y \in Y$, $a(x)$ and $b(x)$ as in (105) and (106) solve the systems (72b, 72a). □

8.2 Invertability of K, M

We want to proof the claims of Proposition 10; hence we want to proof that both K, M as in (73) are invertible. We will proof it for the matrix K and $N = 2$.
Recall that

$$K_z = \begin{bmatrix} \frac{k_1}{k_1^2-\rho_1^2} & \frac{k_1}{k_1^2-\rho_2^2} & \frac{k_1}{k_1^2-\rho_3^2} \\ \frac{k_2}{k_2^2-\rho_1^2} & \frac{k_2}{k_2^2-\rho_2^2} & \frac{k_2}{k_2^2-\rho_3^2} \\ 1 & 1 & 1 \end{bmatrix} \tag{139}$$

For convenience define

$$n_j := k_j^2, \quad m_i := \rho_i^2 \text{ for } j = 1, \dots, N, i = 1, \dots, N+1, \tag{140}$$

and for a matrix Q write $|Q|$ for the determinant.
First we notice that

- Because $z \notin \varsigma$ we have
  $n_i = k_i^2 \neq k_j^2 = n_j$ for all $i \neq j$.

- All m_i are distinct since $\rho_i \neq \rho_j$ for all $i \neq j$.

- $n_j - m_i \neq 0$ for all i, j, because of Proposition 6.

We want to show that $\det(K) \neq 0$, hence

$$\det(K) = \begin{vmatrix} \frac{k_1}{k_1^2-\rho_1^2} & \frac{k_1}{k_1^2-\rho_2^2} & \frac{k_1}{k_1^2-\rho_3^2} \\ \frac{k_2}{k_2^2-\rho_1^2} & \frac{k_2}{k_2^2-\rho_2^2} & \frac{k_2}{k_2^2-\rho_3^2} \\ 1 & 1 & 1 \end{vmatrix} = k_1 \cdot k_2 \cdot \begin{vmatrix} \frac{1}{k_1^2-\rho_1^2} & \frac{1}{k_1^2-\rho_2^2} & \frac{1}{k_1^2-\rho_3^2} \\ \frac{1}{k_2^2-\rho_1^2} & \frac{1}{k_2^2-\rho_2^2} & \frac{1}{k_2^2-\rho_3^2} \\ 1 & 1 & 1 \end{vmatrix}, \tag{141}$$

Now using (140) and transposing the matrix, we can rewrite (141) as

$$\det(K) = k_1 \cdot k_2 \cdot \begin{vmatrix} \frac{1}{n_1-m_1} & \frac{1}{n_1-m_2} & \frac{1}{n_1-m_3} \\ \frac{1}{n_2-m_1} & \frac{1}{n_2-m_2} & \frac{1}{n_2-m_3} \\ 1 & 1 & 1 \end{vmatrix} = k_1 \cdot k_2 \cdot \begin{vmatrix} \frac{1}{n_1-m_1} & \frac{1}{n_2-m_1} & 1 \\ \frac{1}{n_1-m_2} & \frac{1}{n_2-m_2} & 1 \\ \frac{1}{n_1-m_3} & \frac{1}{n_2-m_3} & 1 \end{vmatrix}. \tag{142}$$

Switching column one with column three, changes the sign of the determinant, hence

$$\det(K) = -k_1 \cdot k_2 \cdot \begin{vmatrix} 1 & \frac{1}{n_2-m_1} & \frac{1}{n_1-m_1} \\ 1 & \frac{1}{n_2-m_2} & \frac{1}{n_1-m_2} \\ 1 & \frac{1}{n_2-m_3} & \frac{1}{n_1-m_3} \end{vmatrix}. \tag{143}$$

It is now possible to subtract row one to row 2 and 3, without changing the determinant,

$$\det(K) = -k_1 \cdot k_2 \cdot \begin{vmatrix} 1 & \frac{1}{n_2-m_1} & \frac{1}{n_1-m_1} \\ 0 & \frac{1}{n_2-m_2} - \frac{1}{n_2-m_1} & \frac{1}{n_1-m_2} - \frac{1}{n_1-m_1} \\ 0 & \frac{1}{n_2-m_3} - \frac{1}{n_2-m_1} & \frac{1}{n_1-m_3} - \frac{1}{n_1-m_1} \end{vmatrix}, \tag{144}$$

and noticing that

$$\frac{1}{n_j - m_i} - \frac{1}{n_j - m_1} = \frac{m_i - m_1}{(n_j - m_i)(n_j - m_1)}, \tag{145}$$

we write

$$\det(K) = -k_1 \cdot k_2 \cdot \begin{vmatrix} 1 & \frac{1}{n_2-m_1} & \frac{1}{n_1-m_1} \\ 0 & \frac{m_2-m_1}{(n_2-m_2)(n_2-m_1)} & \frac{m_2-m_1}{(n_1-m_2)(n_1-m_1)} \\ 0 & \frac{m_3-m_1}{(n_2-m_3)(n_2-m_1)} & \frac{m_3-m_1}{(n_1-m_3)(n_1-m_1)} \end{vmatrix}. \tag{146}$$

Finally it follows that

$$\begin{aligned} \det(K) &= -k_1 \cdot k_2 \cdot (m_2 - m_1)(m_3 - m_1) \cdot \frac{1}{(n_2 - m_1)(n_1 - m_1)} \begin{vmatrix} 1 & 1 & 1 \\ 0 & \frac{1}{n_2-m_2} & \frac{1}{n_1-m_2} \\ 0 & \frac{1}{n_2-m_3} & \frac{1}{n_1-m_3} \end{vmatrix} \\ &= \frac{-k_1 \cdot k_2 \cdot (m_2 - m_1)(m_3 - m_1)}{(n_2 - m_1)(n_1 - m_1)} \begin{vmatrix} \frac{1}{n_2-m_2} & \frac{1}{n_1-m_2} \\ \frac{1}{n_2-m_3} & \frac{1}{n_1-m_3} \end{vmatrix}. \end{aligned} \tag{147}$$

The matrix

$$Q_1 = \begin{bmatrix} \frac{1}{n_2 - m_2} & \frac{1}{n_1 - m_2} \\ \frac{1}{n_2 - m_3} & \frac{1}{n_1 - m_3} \end{bmatrix} \tag{148}$$

is a Cauchy matrix, hence has non zero determinant. It follows that

$$\det(Q) = \frac{-k_1 \cdot k_2 \cdot (m_2 - m_1)(m_3 - m_1)}{(n_2 - m_1)(n_1 - m_1)} \det(Q_1) \neq 0. \tag{149}$$

The proof is analogous for matrix M. The steps of the proof have to be repeated for each row/column for general N. $\square$

References

[1] S. A. van Gils, S. G. Janssens, Y. A. Kuznetsov, and S. Visser, " On local bifurcations in neural fields models with transmission delays.", *J. Math. Biol.*, vol. 66, no. 4-5, pp.837-87, Mar. 2013.

[2] K. Dijkstra, S. A. Van Gils, S. G. Janssens, Y. A. Kuznetsov, and S. Visser, "Pitchfork-Hopf bifurcations in 1D neural field models with transmission delays", *Phys. D. Non-linear Phenom.*, vol. 297, pp. 88-101, 2015. 2, 85-104.

[3] O.Diekmann, S.A. van Gils, S.M. Verduyn Lunel, H.-O- Walther, Delay Equations: Functional, Complex, and Nonlinear Analysis, in. Applied Mathematical Science, vol. 110, Springer Verlag, New York, 1995.

[4] K.-J. Engel, R. Nagel, *One-Parameter Semigroups for Linear Evolution Equations*, Graduate Text in Mathematics, vol. 194, Springer-Verlag, New York, 2000.

[5] G. Faye and O. Faugeras, " Some theoretical and numerical results for delayed neural field equations", *Phys. D. Nonlinear Phenom.*, vol. 239, no. 9, pp. 561-578. May 2010.

[6] G. Granier, J.M.A.M. van Neerven, "Adjoints of semigroups acting on vector-valued function spaces", *Israel J. Math.* 77(3)(1992) 305-333.

[7] S.A. Van Gils, S.G. Janssens, "A class of abstract delay differential equations in the light of suns and stars", *Tech. report*, Dep. of Mathematics, University of Twente, 2012.

[8] R. Veltz and O. Faugeras, "Stability of the stationary solutions of neural field equations with propagation delays", *Journal of mathematical Neuroscience*, vol. 1, no. 1, 2011.

[9] J. Guckenheimer, P. Holmes, 'Nonlinear Oscilations, Dynamical Systems, and Bifurcation of Vector Fields', *Applied Mathematical Sciences*, vol. 42, Springer,

New York, 1983.

[10] K. Engelborghs, T. Luzyanina, D. Roose, "Numerical bifurcation analysis of delay differential equations using DDE-BIFTOOL", ACM Trans. Math. Software 28 (2002) 1-21.

[11] H.C. Wilson, J.D. Cowan, "Excitatory and inhibitory interactions in localized populations of model neurons". *Biophys. J.* 12, 1-24, 1972.

[12] H.C. Wilson, J.D. Cowan, "A mathematical theory of the functional dynamics of cortical and thalamic nervous tissue". *Kybernetik* 13,55-80, 1973.

[13] P.L. Nunez, "The brain wave equation: a model for the EEG". *Math. Biosci.* 21, 279-297, 1974.

[14] S. Amari, "Dynamics of pattern formation in lateral-inhibitory type neural fields". *Biol. Cybern.* 27, 77-87, 1977.

[15] F. Lopes Da Silva, W. Blanes, S. N. Kalitzin, J. Parra, P. Suffczynski, D. N. Velis, "Epilepsies as dynamical diseases of brain systems: basic models of the transition between normal and epileptic activity". *Epilepsia* 44 (12 Suppl.), 72-83, 2003.